The biophysical channels of climate impacts

Romain Fillon*

October 16, 2024

Abstract

To what extent does regional economic activity shape regional climate impacts? Land use land cover (LULC) changes with regional economic activity through agricultural and urban land demands. At the regional scale, LULC changes affect climate impacts through changes in albedo, evapotranspiration and roughness length, i.e. biophysical channels. These spatially heterogeneous regional feedbacks have so far been neglected in the quantitative spatial literature assessing the economic consequences of climate change. Indeed, the literature focuses on the biogeochemical channel from global carbon concentration. Accounting for this additional biophysical feedback between regional economic activities and regional climate change yields important welfare implications for both adaptation and mitigation, as the biophysical feedbacks change temperature impacts and interact with regional adaptation decisions. I build a dynamic-spatial sectoral equilibrium model to understand the impact of this omitted nonlinear physical mechanism and take the model to the data at the global gridded 1° resolution to quantify its magnitude along 'middle-of-the-road' SSP2-4.5 with agents that adapt to climate impacts through migration and trade. I leverage recent advances in the climate adaptive response literature to estimate model-consistent dose-response functions of regional amenities and sectoral productivities to regional annual distributions of daily mean surface temperatures from the equilibrium conditions of the model. Im my baseline SSP2-4.5 simulation, without biophysical impacts, almost all locations experience negative welfare changes from nonlinear regional intra-annual warming patterns interacted with nonlinear binned damage patterns: there are no benefits to be expected from climate change in the Northern Hemisphere. Adding biophysical channels, i.e. a non-linear and time-varying downscaling from global to regional temperature distributions, accounts for 2.4% of the aggregate biogeochemical welfare impacts of climate change. Both biogeochemical and biophysical climate impacts are regressive, decreasing with 2015 income per capita levels.

Keywords: environmental policy, spatial integrated assessment models, endogenous adaptation, land use land cover, albedo, evapotranspiration, roughness, downscaling.

*Université Paris-Saclay (Centre International de Recherche sur l'Environnement et le Développement - CIRED & Paris-Saclay Applied Economics - PSAE)

1 Introduction

'Any local land changes that redistribute energy and water vapour between the land and the atmosphere influence regional climate (biophysical effects, high confidence)' (IPCC).

Uncertainties about changes in land conditions originating from anthropogenic land uses have become a major concern, as highlighted by IPCC in its 2019 special report on climate change and land (Masson-Delmotte et al., 2019). Changes in land conditions have for instance a major impact on biodiversity and contribute to global climate change through carbon releases or by reducing land carbon storage potential. But in this study, I focus on the *regional biophysical climate impacts* of changes in regional land conditions. These biophysical impacts are not driven by carbon emissions but by changes in albedo, evapotranspiration and soil roughness, which can reduce or accentuate regional warming (Georgescu et al., 2011; Alkama and Cescatti, 2016) depending on the location and season (Duveiller et al., 2018b).

To my knowledge, economists usually omit these mechanisms in their assessments of climate impacts: they focus on the biogeochemical channel of global carbon emissions. For instance, in the burgeoning field of spatial integrated assessment modelling (Desmet and Rossi-Hansberg, 2024), regional temperatures at location r and time t are inferred from global average temperatures through statistical downscaling, also called pattern scaling (Santer et al., 1990). As depicted in Fernández-Villalverde et al. (2024), pattern-scaling suggests a simple functional relation such as: $T_t(r) = f(T_t^A) + \eta_t(r)$, where local temperature $T_t(r)$ at grid cell r and time t is a response to global average temperature T_t^A indicated by $f(.)$ and a stochastic local residual temperature variability term $\eta_t(r)$. The stochastic process that determines the distribution of local residual $\eta_t(r)$ is assumed to be *stationary* and *exogenous* to regional economic activities. In this work, I reconsider these two assumptions. As our understanding of the mechanisms through which human activities and climate impacts interact goes to finer spatial resolution, I investigate the heterogenous endogenous dynamic biophysical regional impacts

and their interactions with adaptation and economic decisions. I quantify how much the regional biophysical channels driven by land use land cover (LULC) changes matter along 'middle-of-the-road' Shared Socioeconomic Pathways (SSP) 2-4.5.

Human-induced LULC changes affect regional climate through three key biophysical channels: change in albedo, change in evapotranspiration and change in surface roughness length. Albedo is the fraction of solar radiation reflected by a surface. Evapotranspiration is the combined process of evaporation from the Earth's surface and transpiration from vegetation. Roughness length refers to the measure of a surface's roughness, which influences how air moves above that surface. Surfaces with less albedo, e.g. because of urbanization, absorb more solar radiation which leads to higher temperatures as more solar energy is converted to heat in these areas. Evapotranspiration decreases in a given location, e.g. because of deforestation, mean that less water is evaporated from surfaces, requiring less energy to change state from liquid to gas while this energy is usually drawn from the environment, cooling both the surface and the surrounding air. The decrease in evapotranspiration can thus bring regional temperature increases. Rough surfaces, such as forests or areas with rugged topography, can slow down air movement, thereby promoting the cooling of local temperatures. Smoother agricultural and urban areas, on the other hand, can reduce frictional drag on the air, allowing warmer air from surrounding regions to flow into these areas. These three biophysical mechanisms are affected by changes in physical land surface characteristics, especially human-driven land use land cover changes: there are regional feedbacks between human activity and these biophysical channels. The two key human drivers that I study here are changes in agricultural and urban land demands.

The biophysical channels matter for climate economics for two main reasons. First, there are heterogeneous LULC changes to be expected around the world depending on current LULC, future economic growth, structural change, demography and climate impacts. Second, these biophysical channels interact with adaptation decisions. For

instance, population concentration in areas that are less affected by climate impacts drives urban land demand and changes in regional biophysical impacts that can reduce the aggregate benefits of migration and change the distributional impacts of the climate burden between regions. This might matter if climate change and population growth have their most damaging effects in similar places (Henderson et al., 2024). Heterogeneous climate impacts and economic dynamics in different regions of the world and in different sectors are driving changes in sectoral specializations, for example by shifting the optimal climate zones for agricultural activities or changing relative prices. These changes in sectoral specialization come with changes in agricultural land extent which have biophysical impacts. The biophysical channels might reduce or increase the benefits of regional adaptation expected from structural change.

There are large heterogeneities in the impacts of these biophysical feedbacks, both physical and socioeconomic. On the one hand, there are spatial and temporal heterogeneities in the biophysical mechanisms. Indeed, observations show that biophysical channels do not have the same impact over different periods of the year (Duveiller et al., 2020). Furthermore, biophysical channels can vary in sign and magnitude depending on regional background climate (Duveiller et al., 2018b): land use changes, for instance from forest to grassland, bring conflicting changes in albedo (increase) and evapotranspiration (decrease). These conflicting changes may lead to cooling or warming depending on which process dominates, which depends on local climate background. Huang et al. (2020) explore this spatial heterogeneity within Europe. On the other hand, there are large spatial and temporal heterogeneity in the socio-economic drivers of land use land cover changes bringing biophysical impacts, because there are various land use land covers today and future land use land cover changes. Different paths of urbanization are to be expected in different parts of the world, depending on demography, economic growth and climate impacts, among others drivers (UN World Urbanization Prospects). Different paths of agricultural land use land cover changes

will also occur depending on structural change, food needs and heterogeneous impacts of climate change on agricultural yields, *etc.* (Future of Food and Agriculture, UN FAO). The interaction between these sources of spatial and temporal heterogeneity, both biophysical and socioeconomic, might even increase the divergence between different locations over the world.

In this paper, I estimate the aggregate and distributional welfare impacts of the biophysical channels of climate impacts along SSP2-4.5. First, I match LULC scenario from LUMIP MESSAGE-Globiom along SSP2-4.5 with Duveiller et al. (2018b) and Zhou et al. (2022) gridded estimates of the historical impact of LULC changes on daily mean daytime and nighttime land surface temperatures. More specifically, I compute the mean impact over thirteen Köppen-Geiger climate zones as the regional biophysical feedbacks depend on background climate. I then use a gridded linear relation between daytime and nighttime land surface temperatures and daily mean surface temperature (Hooker et al., 2018), a metric adapted to the measure of climate impacts on economic activities. This procedure allows me to build a reduced-form representation of the regional biophysical feedbacks that can be projected using anticipated gridded changes in Köppen-Geiger zones along SSP2-4.5 (Beck et al., 2023) and changes in LULC.

I build a two-sectors (agricultural sector and all other sectors), dynamic quantitative spatial equilibrium model (Eaton and Kortum, 2002; Redding and Rossi-Hansberg, 2017) where locations differ in regional annual distribution of mean daily surface temperature, sectoral productivities, amenities, bilateral trade and migration costs. Productivities represent features that make different regions more or less attractive in terms of the costs of production, which may include natural advantages (such as proximity of natural resources) or induced advantages (such as infrastructure). Regional amenities capture characteristics of each location that make them more or less desirable places to live. Workers in each location have preference for regional amenities and consume a

variety of horizontally differentiated goods. They experience idiosyncratic preference shocks. Workers are mobile across locations but face time-invariant migration costs. Their migration decisions are simplified *a la* Desmet et al. (2018) to make the 1° gridded model tractable. I use Caliendo et al. (2019); Kleinman et al. (2023) dynamic exact hat algebra technique that avoids the shortcomings of regional fundamental amenities estimation. Finally, firms face monopolistic competition without intermediate inputs in the production as in Conte et al. (2021), with time-invariant and symmetric bilateral trade costs that are not sector-specific, and without trade imbalances. I solve the model under the assumption of a stationary equilibrium.

The simulations are done under exogeneous biogeochemical climate change with projections of future distributions of daily mean temperatures taken from the average of bias-adjusted (Lange, 2019) and down-scaled SSP2-4.5 CMIP6 experiments of four Earth System models (ESM) (GFDL-ESM4, IPSL-CM6A-LR, MPI-ESM1-2-HR, MRI-ESM2-0) with the assumption of 2015 fixed land use. Biophysical impacts are added to these exogeneous projections with the implicit assumption of a shape-preserving mean increase in the annual distribution of daily mean temperatures. I could compare these simulations to CMIP projections with exogenous land use change scenarios, but this would lump the two biophysical and biogeochemical effects of land use change together: a change in land use in an ESM leads to a biogeochemical impact via the global carbon cycle (e.g. carbon releases from deforestation), which is not disentangled from the biophysical impact. An important work is done by the LUMIP platform (Lawrence et al., 2016) to disentangle these future land use impacts, especially for deforestation, e.g. in Boysen et al. (2020). But these studies treat the various biophysical impacts in silo, or model them along exogenous scenarios of population, trade, sector specialization, without modeling the endogenous reaction of agents to climate impacts as in the recent quantitative spatial literature (Cruz and Rossi-Hansberg, 2024).

I follow Rudik et al. (2022) and use the equilibrium conditions of the theoretical

model to compute model-consistent dose-response function of regional amenities and sectoral productivities to distortions in the annual regional distribution of daily mean temperatures. The intuition behind this estimation approach is that changes in migration and trade flows allows *ceteris paribus* to identify changes in amenity and sectoral productivity levels. As the dose-response functions are estimated from the equilibrium conditions of the theoretical model, the simulation results reflect the actual welfare impacts of climate change given the model's assumptions regarding macroeconomic dynamics and adaptation decisions. I combine ERA-5 climate reanalysis (Hersbach et al., 2020) of the population-weighted country-level annual distribution of daily mean temperatures with BACI CEPII and Abel and Cohen (2019) datasets on trade and migration flows at the country level. Focusing on the whole shape of the intra-annual distribution of daily mean temperatures rather than an arbitrary moment such as the mean annual temperature (Fillon et al., 2024) allows to capture more complex changes in the high-dimensional temperature vector. The temperature bins allows to capture some of the non-linearity in the climate impacts (Burke et al., 2015).

To what extent does regional economic activity shape regional climate impacts? My quantitative estimation of the biophysical channels of climate change under SSP2-4.5 proceeds in two steps. First, I estimate the aggregate and distributional welfare impacts of the SSP2-4.5 scenario, considering only the carbon cycle—i.e., I ignore the impact of regional economic activity on regional climate change. Then, I assess the aggregate and distributional impacts of SSP2-4.5 with the addition of biophysical channels. Two key conclusions emerge from the first step, where I estimate the baseline impacts of biogeochemical climate change. First, climate change impacts are negative for most regions: by accounting for intra-annual warming patterns and non-linear damage patterns across temperature bins, I find no evidence of benefits from warming in the Northern Hemisphere. The aggregate welfare impact of SSP2-4.5 is, however,

consistent with existing literature; most impacts are driven by the non-linear effect of temperature distortions on sectoral productivities. Second, biogeochemical climate change is regressive: the magnitude of welfare changes under SSP2-4.5 is inversely related to initial income levels in 2015. In the second step, I estimate the impact of biophysical channels. From my simulations, two conclusions arise. First, regional economic activity does indeed influence regional climate impacts and the corresponding welfare changes. On average, this additional biophysical effect accounts for 2.5% of the biogeochemical impacts estimated in the first step. Second, the biophysical impacts vary across both time and space. This heterogeneity is, first, socioeconomic: it depends on scenarios of urban land-use change and the net transitions of shrublands and forests into croplands. It is also climatic: the effect of biophysical channels depends on the climate zone in which a location is situated (e.g., arid, temperate, etc.), with these classifications shifting over time due to global climate change. For some biophysical channels, this heterogeneity is also seasonal, which further strengthens the case for considering the intra-annual distribution of temperatures in the study of climate impacts. In my simulations, I find that most locations experience a negative impact from biophysical channels on welfare under SSP2-4.5. Like the biogeochemical impacts, the biophysical effects are regressive relative to 2015 income levels.

I contribute to three main strands of economic literature. First, I contribute to the growing literature in climate economics using dynamic spatial quantitative equilibrium model to measure the impacts of climate change under endogenous and regional adaptation (Krusell and Smith Jr, 2022; Cruz and Rossi-Hansberg, 2024). In comparison with these spatial integrated assessment models, I do not assume a time-invariant exogenous linear relation between global climate change and regional climate impacts. Indeed, downscaling from global to regional climate change cannot be considered as stable across time and space: it is not exogeneous to our regional economic activities.

Averaging over multiple deterministic draws taking the whole scientific information into account, e.g. similar to work of Desmet et al. (2018) on sea level rise but in application to parametric uncertainty over regional transient climate response to global cumulative emissions, would not allow to capture these nonlinear biophysical mechanisms. Thus, in addition to non-linearities in climate impacts, largely documented since seminal work from Schlenker and Roberts (2009); Burke et al. (2015), i.e. non-linearity in the mapping from a given summary statistics of regional climate change to economic impacts on amenities and productivities, I add physical non-linearities in the mapping from global climate change to regional climate change via endogenous LULC changes. Another venue in this literature is to use actual climate projections (Rudik et al., 2022; Bilal and Rossi-Hansberg, 2023) but this implies that LULC are either assumed time-invariant, or that the biophysical channels of LULC are entangled with their biogeochemical impacts.

Second, I contribute to the literature modelling adaptation which has developed in response to the Lucas critique adressed to the standard climate-economy models (Nordhaus, 2008; Barrage and Nordhaus, 2024): in comparison with previous approaches, I study how adaptation decisions might interact with climate impacts. Thus, I relate to the literature on stuctural transformation under a changing climate (Conte et al., 2021; Albert et al., 2021; Nath, 2022) and urbanization and their interaction with LULC changes (Michaels et al., 2012; Ahlfeldt et al., 2015; Coeurdacier et al., 2022; Eckert and Peters, 2022). I quantify the impact of these sectoral specialization and urbanization changes on regional climates via biophysical mechanisms.

Third, I contribute to the literature studying the interactions betweeen economic activity, land uses and climate impacts. This literature usually focuses on forest covers (Grosset et al., 2023) and micro-scale impacts, for instance health impacts related to urban heat island (Manoli et al., 2019). I extend this literature in three directions: I consider various transitions in land uses (transition from forests to croplands, transition

from shrublands to croplands, transition from non-impervious to impervious surfaces), at the global scale (around 13000 gridded locations) and with larger regional impacts at the 1° gridded resolution, in response to climate scientists' concerns that biophysical impacts are not solely local (Duveiller et al., 2018b; Chakraborty and Qian, 2024).

2 Motivation

2.1 Regional biophysical channels and their impacts

2.1.1 Impact of regional agricultural land demand on regional climate

Changes in agricultural LULC have heterogeneous impacts on regional climates and depending on the season. Duveiller et al. (2018a) provide gridded estimates of climate impacts stemming from regional transitions from and to croplands at 1° spatial resolution. While the authors also provide estimates for grasslands, they do not differentiate between rangelands grazed by domestic livestock and other uses. I thus focus on changes in croplands without considering pastures. I compute the mean temperature impact of these land transitions over Köppen-Geiger climate zones because biophysical impacts depend on regional climate backgrounds (Duveiller et al., 2020). In table (1), I give the distribution of change in mean daily surface temperature observed for two LULC transitions in all Köppen-Geiger climatic zones: transition from forests to croplands and transition from shrublands to croplands. I convert daytime and nighttime land surface temperatures to mean two-meters surface temperature using gridded linear relations uncovered in Hooker et al. (2018).

Koppen-Geiger climate zone	Forests to Croplands	Shrublands to Croplands
Arid, desert	- / -	0.0108/0.0169°C
Humid continental	0.0078/0.0015°C	-0.0102/0.0018°C
Humid subtropical	0.002/0.0017°C	0.0046/-0.0021°C
Mediterranean	0.0029/0.0003°C	- / -
Mediterranean continental	-0.0087/0.0007°C	-0.0007/-0.0025°C
Oceanic	-0.0013/-0.0038°C	0.0098 / - °C
Semi-Arid	-0.0015/0.0013°C	0.0043/0.009°C
Subarctic	-0.0037/0.0005°C	-0.0048/0.0028°C
Tropical, Monsoon	0.0022/0.0001°C	0.0032/-0.0033°C
Tropical, Rainforest	0.0017/0.003°C	0.0043/-0.0079°C
Tropical, Savannah	-0.0048/-0.0004°C	0.0026/0.0037°C
Tundra	0.0022/0.0104°C	0.0148/-0.0016°C

Table 1: Change in monthly (January/July for illustration) mean daily surface temperature (in °C) for various Köppen-Geiger climatic zones for a 1% absolute change in land use for two net transitions of interest: from forests to croplands, from shrublands to croplands. 1% absolute change over 1° gridded regions represents around 123km^2 at Equator and 87km^2 on the French mainland. Data is missing for some combinations.

2.1.2 Impact of regional urban land demand on regional climate

Changes in urban LULC have an impact on regional climates (Zhou et al., 2022). To my knowledge, most studies focus on local urban heat islands effect in cities while I refer to all global artificial impervious surfaces as these areas have temperature impacts that go beyond local effects (Chakraborty and Qian, 2024). Past decades have seen large changes in global artificial impervious surfaces. Zhou et al. (2022) give gridded regional climate impacts of global artificial impervious surfaces extension at 50km x 50 km resolution. More specifically, the authors give the change in urbanization over 1985 to 2015 and the change in daytime and nighttime land surface temperature (LST)

due to increase in urbanization over the same period. I convert daytime and nighttime LST to mean two-meters surface temperature using Hooker et al. (2018). I compute the mean impact over Köppen-Geiger climate zones because I expect the impact to depend on regional climate background as for urban heat islands (Zhao et al., 2014). In table (2), I give the distribution of annual mean daily temperature changes from a 1% increase in impervious surfaces.

Mean change	Koppen-Geiger climate zone
0.0077°C	Arid, desert
0.0096°C	Humid continental
0.0115°C	Humid subtropical
0.0103°C	Mediterranean
0.0083°C	Mediterranean continental
0.0106°C	Oceanic
0.0076°C	Semi-Arid
0.0068°C	Subarctic
0.0108°C	Tropical, Monsoon
0.0077°C	Tropical, Rainforest
0.0123°C	Tropical, Savannah
0.0114°C	Tundra

Table 2: Change in annual mean daily surface temperature (in °C) for various Köppen-Geiger climatic zones for a 1% absolute change in impervious surfaces over 1° gridded regions, i.e. around 123km^2 at Equator and 87km^2 on the French mainland.

In order to use these estimates for simulations using distributions of daily mean temperatures, I make two assumptions. First, I assume homogeneity in the shift in distribution of daily mean temperatures within each year (urban land) and each month (croplands). Second, I assume that the change computed for each Köppen-Geiger zone holds in the future under changing climate for the same climatic zone.

2.1.3 Köppen-Geiger climates

I plot the 2015 distribution of Köppen-Geiger climate zones.

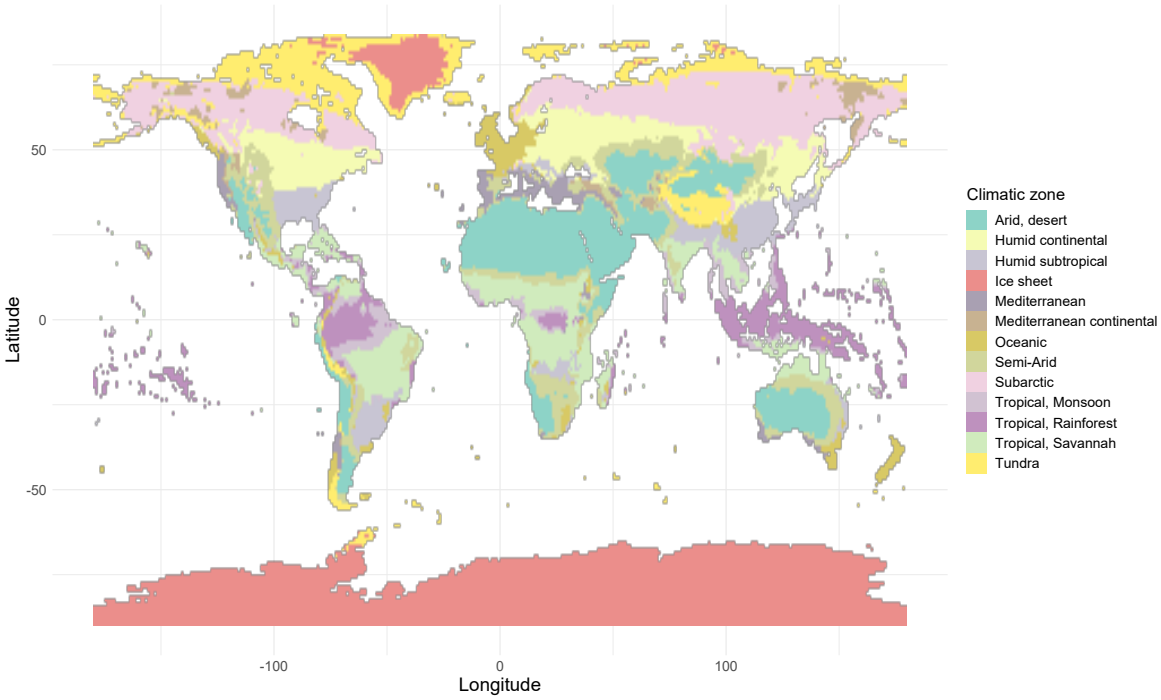

Figure 1: 13 Köppen-Geiger climate reference regions in 2015.

According to Beck et al. (2023), 8% of current land surface will transition to another Koppen-Geiger region along SSP2-4.5. Thus, I can not use fixed current Koppen-Geiger zone while the sign and magnitude of the biophysical channel stemming from land use land cover changes depend on it. I use Beck et al. (2023) data to project in which Köppen-Geiger zone each 1° grid cell will be along SSP2-4.5. Regions that change affiliation between 2015 and 2100 are:

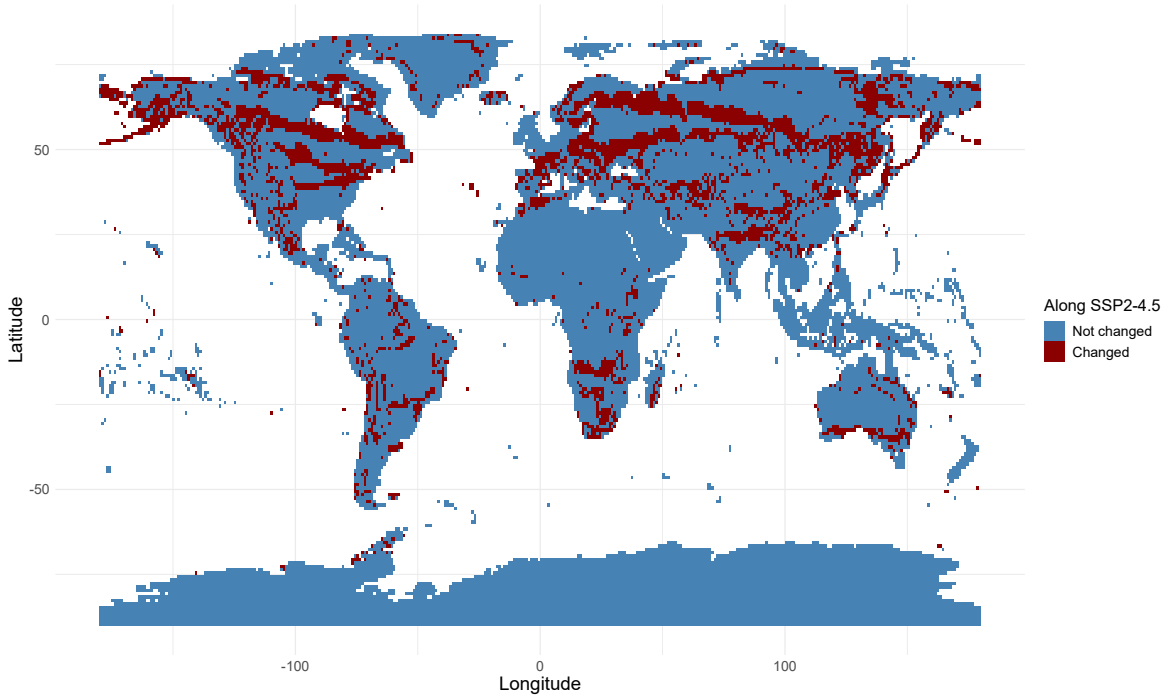

Figure 2: 1° locations who change Köppen-Geiger classification between 2015 and 2100 under SSP2-4.5.

2.2 Impact of economic activities on LULC changes

Once I have retrieved these estimates linking LULC to biophysical impacts, I map changes in economic activities to LULC changes. In table (3), I give summary statistics for the distribution of cumulative net transitions from forests to croplands, from rangelands[1] to croplands, from non-impervious to impervious surfaces from 2015 to 2100 under SSP2-4.5 in MESSAGE-Globiom (Hurtt et al., 2020), stored on the LU-MIP platform.

[1]As a first approximation, I assume that biophysical channels estimated in Duveiller et al. (2018b) for generic shrublands applies to the MESSAGE Globiom category of rangelands that does not include domestic pastured grasslands. I could disentangle further between savannas and shrublands.

Quantiles	Forests to croplands	Rangelands to croplands	Non-urban to urban
0%	-56.88	-27.19	-4.65
20%	-0.49	0.00	0.00
40%	0.19	0.01	0.03
60%	1.01	0.17	0.13
80%	3.60	0.83	0.51
100%	63.96	43.36	19.19

Table 3: Cumulative net change (as a share of total cell extent, in %) between 2015 and 2100 in LUMIP MESSAGE-Globiom SSP2 4-5 for the 1° gridded locations used in the simulations, from forests to croplands (left), from rangelands to croplands (middle), from non-impervious to urban impervious surfaces (right).

Interacted with biophysical changes from tables (1) and (2), these LULC changes have a heterogeneous impact on the future annual distributions of daily mean temperatures around the world and over time. These dynamic biophysical impacts affect the future distribution of economic activities, populations and welfare throughout the world in a way that is omitted from estimates of climate change impacts of the quantitative spatial literature that uses time-invariant linear temperature down-scaling. Model that use projections from CMIP6 earth system models either assume fixed land use or use projections forced with direct human forcing such as land use changes which do not differentiate between the various channels by which land and other elements of the SSP affect climate, e.g. the specific biophysical channels that we study here.

I have retrieved estimates linking economic activity to heterogeneous biophysical impacts at the regional scale *via* changes in agricultural and urban land demands. I build a spatial sectoral equilibrium model to understand how these regional feedbacks interact with standard biogeochemical climate impacts and regional adaptation decisions. I quantify how these dynamic mechanisms shape the distribution of economic

activity, population and climate impacts along SSP2-4.5.

3 Theoretical Model

3.1 Households

3.1.1 Preferences and migrations

Period utility of a worker j who resides in location r at t is multiplicative in four elements: the level of regional amenities $a_t(r)$ that captures how valuable living in a given location is other things being equal, the consumption of goods $C_t(r)$, an individual-specific idiosyncratic preference shock ϵ_t^j, drawn from a Fréchet distribution (i.i.d. across locations, individuals, and time) with a shape parameter that equals the elasticity of migration to real income, and the cost of migrating from location r in period s - 1 to a location r in period s.

$$U_t^j(r) = a_t(r)C_t(r)\epsilon_t^j(r)\Pi_{s=1}^t m(r_{s-1}, r_s)^{-1} \tag{1}$$

Dynamic migration decisions are simplified to static decisions as in Desmet et al. (2018), so that: $m(s,r) = m_1(s)m_2(r)$ and $m(r,r) = 1$, i.e. there is no cost to staying in the same place and the utility discount from migration is the product of origin and destination-specific discounts. This yields that $m_2(r) = 1/m_1(r)$, i.e. the cost of entering a location is fully compensated by the benefit from leaving. This symmetry assumption allows to reduce the dimension of my spatial dynamic migration problem with many locations and makes it tractable at the global 1° gridded scale with standard resolutions methods.

3.1.2 Consumption and income

I assume a Cobb-Douglas preference structure between goods and a Spence-Dixit-Stiglitz preference structure between horizontally differentiated varieties for each good, with $1/(1-\rho)$ the elasticity of substitution between goods. I assume $\rho > 1$ in my setting, so that varieties are substitutes. χ_i is the fixed share of good i in the worker's expenditure. Consumption of goods at time t in location r writes:

$$C_t(r) = \Pi_{k=1}^{K} \left[\int_0^1 c_t^{k\omega}(r)^{\rho} d\omega \right]^{\frac{\chi_i}{\rho}} \tag{2}$$

Workers in location r supplies one unit of labor inelastically and receive wage $w_t(r)$ in location r and sector k in which they live in period t so that total income is: $y_t(r) = L_t(r)w_t(r)/\left(\Pi_{k\in K} P_t^k(r)^{\chi^k}\right)$ where $\Pi_{k\in K} P_t^k(r)^{\chi^k}$ is the ideal price index over K sectors. There is no money lending, so every period agents fully consume their income and $C_t(r) = y_t(r)$. In each location, there is immobile and non-accumulating capital which I call regional sectoral structures H_t^k as in Caliendo et al. (2019). H_t^k is assumed to be fixed over time and generate a rent that is fully used to maintain these structures.

3.1.3 Regional amenities

Following Desmet et al. (2018), idiosyncratic non-weather time-invariant fundamental regional amenities $\bar{a}_t(r)$ are affected by congestion, with $L_t(r)$ the population in location r at time t and λ the congestion elasticity of amenities to population density. Following Rudik et al. (2022), regional amenities $a_t(r)$ are multiplicatively separable in a weather component $exp(f[T_t(r); \zeta_a])$, where $T_t(r)$ is a vector of weather variables that summarizes the high-dimensional climate, f an arbitrary function taken over this distribution (e.g. orthogonal polynomials, cubic splines) and ζ_a the set of parameters to be estimated that governs how the weather vector affects regional amenities non-linearly. In my benchmark estimation for ζ_a, I use third-degree orthogonal poly-

nomials for smoothing across the annual distribution of daily mean temperatures with 1°C temperature bins. Regional temperature is a function of the biogeochemical cycle, taken from exogeneous SSP projections, and the biophysical channel driven by endogenous LULC changes. Regional amenity writes: $a_t(r) = \bar{a}_{t-1}(r)L_t(r)^{-\lambda}exp\left(f[T_t(r);\zeta_a]\right)$. Desmet et al. (2018) show that $u_t(r) = a_t(r)y_t(r)$ fully summarizes how individuals value the amenity and production characteristics of a location. But uncovering the initial distribution of non-weather time-invariant amenities $\bar{a}_t(r)$, i.e. what makes a location attractive irrespective of economic activity, is challenging[2]. I use Caliendo et al. (2019)'s dynamic exact hat algebra approach to get around this issue.

3.1.4 Dynamic exact hat algebra and population dynamics

Following Desmet et al. (2018), the share of the population in location r that moves to location s from t-1 to t among all possible locations N is:

$$\mu_t(rs) = \frac{u_t(s)^{1/\Omega} m_2(rs)^{-1/\Omega}}{\sum_{n\in N} u_t(n)^{1/\Omega} m_2(rn)^{-1/\Omega}} \tag{3}$$

Following Caliendo et al. (2019) and Balboni (2019), I write the change in the bilateral matrix of migration flows in dynamic exact hat algebra:

$$\dot{\mu}_{t+1}(rs) = \frac{\mu_{t+1}(rs)}{\mu_t(rs)} = \frac{\dot{u}_{t+1}(s)^{1/\Omega}}{\sum_{n\in N} \mu_t(rn)\dot{u}_{t+1}(n)^{1/\Omega}} \tag{4}$$

And, as the idiosyncratic non-weather dependent part of regional amenities are constant in time: $\dot{u}_{t+1}(r) = \dot{y}_{t+1}(r)\dot{L}_{t+1}(r)^{-\lambda}exp\left[f(T_{t+1}(r),\zeta_a) - f(T_t(r),\zeta_a)\right]$. Once I have migration flows, I build population dynamics for each location, accounting for exogenous birth and death rates from SSP projections without migrations. In comparison with Cruz (2021), I do not model endogenous fertility and death rates. Population

[2]Attempts include Desmet et al. (2018), who use model inversion to recover these initial amenities with subjective well-being survey from the Gallup World Poll, and Cruz and Rossi-Hansberg (2024) with Kummu et al. (2018)'s gridded data on reconstructed human development index.

dynamics, with $L_t(r) = \sum_{k \in K} L_t^k(r)$, writes:

$$L_{t+1}^k(r) = (b_{t+1}(r) - d_{t+1}(r))L_t^k(r) + \sum_{l=0, l \neq r}^{N} \sum_{k \in K} \mu_{t+1}(lr L_t^k(l) - \sum_{l=0, l \neq r}^{N} \sum_{k \in K} \mu_{t+1}(rl) L_t^k(r) \tag{5}$$

Thus, to recover the full dynamics of population under changing climate, I need gridded projections for births and deaths rates along SSP2-4.5 without migration, a guess for the change in utility, observed initial bilateral matrix of migration flows $\mu_0(rs)$, initial distribution of sectoral population $L_0^k(r)$ and the gridded path of the future annual distributions of mean daily temperatures. Then, period by period, I can recover migration flows, without information on the initial distribution of non-weather time-invariant regional amenities.

3.2 Production

3.2.1 Profit maximization

I assume that each 1° economy produces a continuum of varieties ω in sector k with a Cobb-Douglas production technology. A firm produces $q_t^{k\omega}(r)$ units of good from sector k and variety ω in location r at t with technology $q_t^{k\omega}(r) = z_t^{k\omega}(r) L_t^{k\omega}(r)^{\mu^k} H_t^{k\omega}(r)^{1-\mu^k}$ and constant returns to scale with two factors of production, regional sectoral structures and labour, $H_t^{k\omega}(r)$ and $L_t^{k\omega}(r)$. I assume away inter-sectoral intra-location trade, i.e. intermediate inputs in the production function. $z_t^{k\omega}(r)$ is a location-sector-variety random variable drawn independently for each triplet (r, k, ω) from a Frechet distribution: $F_t^{k\omega}(r) = exp\left[-Z_t^{k\omega}(r)(z)^{-\theta^k}\right]$. Firms are perfectly competitive. Taking all prices as given, a firm producing variety ω of good in location r and sector k chooses inputs to maximize static profits: $\Pi_t^{k\omega}(r) = p_t^{k\omega}(r) q_t^{k\omega}(r) - w_t(r) L_t^{k\omega}(r) - R_t(r) H_t^{k\omega}(r)$, where $p_t^{k\omega}(r)$ is the price of variety ω of good produced and sold in location r and sector k and input costs are not sector-specific. The unit price of an input bundle in location

r, i.e. the marginal cost of production, with κ^k the sector-specific constants, writes: $x_t^k(r) = \kappa^k(w_t(r))^{\mu^k}(R_t(r))^{1-\mu^k}$. First-order conditions of the firm's profit maximization problem for sector k, time t and location r relate regional structure rents to wages and sectoral labour employment levels $R_t^k(r)H_t^k(r) = w_t(r)\frac{1-\mu^k}{\mu^k}L_t^k(r)$.

3.2.2 Regional productivities

As for amenities, productivity Z in each location r is multiplicatively separable in a vector of weather variables, where $\bar{Z}$ is non-weather base productivity : $Z_t^k(r) = \bar{Z}_t^k(r)exp\left(g[T_t(r);\zeta_z]\right)$. Non-weather productivity $\bar{Z}_{rt}^k$ grows exogenously[3] at a rate ϕ that is not sector-specific. In each location, the vector of temperatures T depend on both biogeochemical and biophysical channels. In hat algebra, productivity changes in location i, sector k and time t write $\dot{Z}_{t+1}^k(r) = \phi exp\left(g[T_{t+1}(r);\zeta_z] - g[T_t(r);\zeta_z]\right)$, where ζ_z is a set of parameters to be estimated that govern how productivity changes non-linearly across temperature bins and g an arbitrary function over the regional annual distribution of daily mean temperatures $T_t(r)$.

3.2.3 Trade, prices, market clearing

I use time-invariant iceberg trade costs τ_{rs} from location r to s among N locations. The trade costs are not specific to sectors. Following Eaton and Kortum (2002), trade shares write:

$$\lambda_t^k(rs) = \frac{Z_t^k(s)\left(x_t^k(s)\tau_{rs}^k\right)^{-\theta^k}}{\sum_l^N Z_t^k(l)\left(x_t^k(l)\tau_{rl}^k\right)^{-\theta^k}} \tag{6}$$

where $\lambda_t^k(rs)$ is the share of expenditures from region s and sector k in region r total expenditures from sector k. The price index for industry k in region r is therefore, with

[3]Spatial diffusion models might not reflect how innovation spreads (Audretsch and Feldman, 1996).

Γ^k a constant and $1 + \theta^k > \sigma^k$:

$$P_t^k(r) = \Gamma^k \left(\sum_{l=1}^{N} Z_t^k(l) [x_t^k(l) \tau_{rl}^k]^{-\theta^k} \right)^{-1/\theta^k} \tag{7}$$

Finally, market clearing at t in r means that labor income in sector k equals the labor share of global expenditures from location r and sector k product: $w_t(r) L_t^k(r) = \chi^k \sum_l^N \lambda_t^k(lr) \left[w_t(l) L_t^k(l) \right]$, with χ^k the share of goods from sector k in location's expenditures. Combining this equation for both sectors yield a clearing equation from which guess on wage can be updated for the period equilibrium.

3.2.4 Production in exact hat algebra

In exact hat algebra, change in unit price of an input bundle is:

$$\dot{x}_{t+1}^k(r) = (\dot{w}_{t+1}(r))^{\mu^k} (\dot{R}_{t+1}^k(r))^{1-\mu^k} \tag{8}$$

and from equation on rents I have that: $\dot{R}_{t+1}^k(r) = \frac{\dot{w}_{t+1}(r)}{\dot{H}_{t+1}^k(r)} \dot{L}_{t+1}^k(r)$ and $\dot{H}_{t+1}^k(r) = 1$. Finally, in dynamic hat algebra, change in price index writes:

$$\dot{P}_{t+1}^k(r) = \left(\sum_{l=1}^{N} \lambda_t^k(rl) \dot{Z}_{t+1}^k(l) [\dot{x}_{t+1}^k(l)]^{-\theta^k} \right)^{-1/\theta^k} \tag{9}$$

Change in trade flows writes:

$$\dot{\lambda}_{t+1}^k(rs) = \frac{\dot{Z}_{t+1}^k(s) \left(\dot{x}_{t+1}^k(s) \right)^{-\theta^k}}{\sum_l^N \lambda_t^k(rl) \dot{Z}_{t+1}^k(l) \left(\dot{x}_{t+1}^k(l) \right)^{-\theta^k}} = \dot{Z}_{t+1}^k(s) \left(\frac{\dot{x}_{t+1}^k(s)}{\dot{P}_{t+1}^k(r)} \right)^{-\Theta^k} \tag{10}$$

3.3 Estimation of dose-response functions

Climate impacts now come into play. They multiplicatively affect sectoral productivity and amenities, thereby distorting market clearing and the distribution of populations

and economic activities over time. I follow the insights of Eaton and Kortum (2002) that trade flows contain information on productivity, and insights from Rudik et al. (2022) that migration flows contain information on amenity value. I use the equilibrium conditions of the model governing bilateral migration and trade flows to estimate impact of regional climates on regional amenities and productivities. I follow a procedure close to Rudik et al. (2022) with more countries, different datasets and relative levels of temperature distributions winsoring rather than absolute temperature bounds. This procedure guarantees internal validity of my estimates, i.e. model-consistent amenity and productivity dose-response functions. Indeed, I leverage the model's structure at equilibrium, so that the non-linear dose-response functions account for the dynamic and spatial interactions modelled in my framework. Finally, the estimates are more robust to spatial autocorrelation than standard panel fixed-effect approaches.

3.3.1 Regional amenities

The intuition behind this estimation is that an observed change in bilateral migration flows, controlling for changes in relative populations and outputs, migration costs and country and time fixed effects, as well as differences in annual distribution of daily mean temperatures between countries allows to identify nonlinear impacts of an additional day in a temperature bin on amenity value. Indeed, the model at equilibrium yields:

$$log\left(\frac{\mu_t(rs)}{\mu_t(rr)}\right) = \frac{1}{\Omega} log\left(\frac{\bar{a}_{t-1}(s)}{\bar{a}_{t-1}(r)}\right) - \frac{\lambda}{\Omega} log\left(\frac{L_t(s)}{L_t(r)}\right) + \frac{1}{\Omega} log\frac{y_t(s)}{y_t(r)} + \frac{1}{\Omega} log(m(r,s)) + \frac{1}{\Omega}\left(f(T_t(s),\zeta_a) - f(T_t(r),\zeta_a)\right) \tag{11}$$

The left hand side is the ratio of households who move to location s (r, s) versus stay in the original location r (r, r) from t-1 to t. The right side has five components. The first component is the ratio of non-weather idiosyncratic amenities, that are time-invariant and captured by a fixed effect in the regression. The second and third components are the difference in population and output. The fourth component is the

difference in migration costs, also time-invariant and captured by the origin-destination fixed effect. Finally, I estimate the non-linear marginal impact of an additional day in a temperature bin on amenity values, ζ_a, from $f(T_t(s), \zeta_a) - f(T_t(r), \zeta_a)$. Arbitrarily, I use a third-degree orthogonal polynomial smoothing across daily 1°C binned mean temperatures for f. For the empirical estimation, I combine Abel and Cohen (2019) data on five-years international migrations flows from 1990 to 2019 with World Bank population and GDP per country estimates and Hersbach et al. (2020)'s climate reanalysis (ERA5) for annual distributions of daily mean surface temperatures. I process the climate reanalysis to aggregate it at the country level, weighting the 0.25° daily mean temperature observations based on population weight in each country. The estimation with Poisson Pseudo Maximum Likelihood and ψ_{rs} an origin-destination fixed effect, is:

$$log\left(\frac{\mu_t(rs)}{\mu_t(rr)}\right) = -\frac{\lambda}{\Omega} log\left(\frac{L_t(s)}{L_t(r)}\right) + \frac{1}{\Omega} log\left(\frac{y_t(s)}{y_t(r)}\right) + \frac{1}{\Omega}\left(f(T_t(s), \zeta_a) - f(T_t(r), \zeta_a)\right) + \psi_{rs} + \delta_t + \epsilon_{rst} \tag{12}$$

with a congestion elasticity of regional amenities to population, $\lambda = 0.32$, taken from Desmet et al. (2018). The regression is done on a distribution that is winsorized at 95% so that the tails of the temperature distribution do not drive results.

Variable	Coefficient	p-value
First-Degree Orthogonal Polynomial	-2.21e-03	3.84e-03
Second-Degree Orthogonal Polynomial	-1.23e-03	3.26e-02
Third-Degree Orthogonal Polynomial	-9.26e-04	2.30e-02
Wald test, joint significance	1.81e+01	4.20e-04

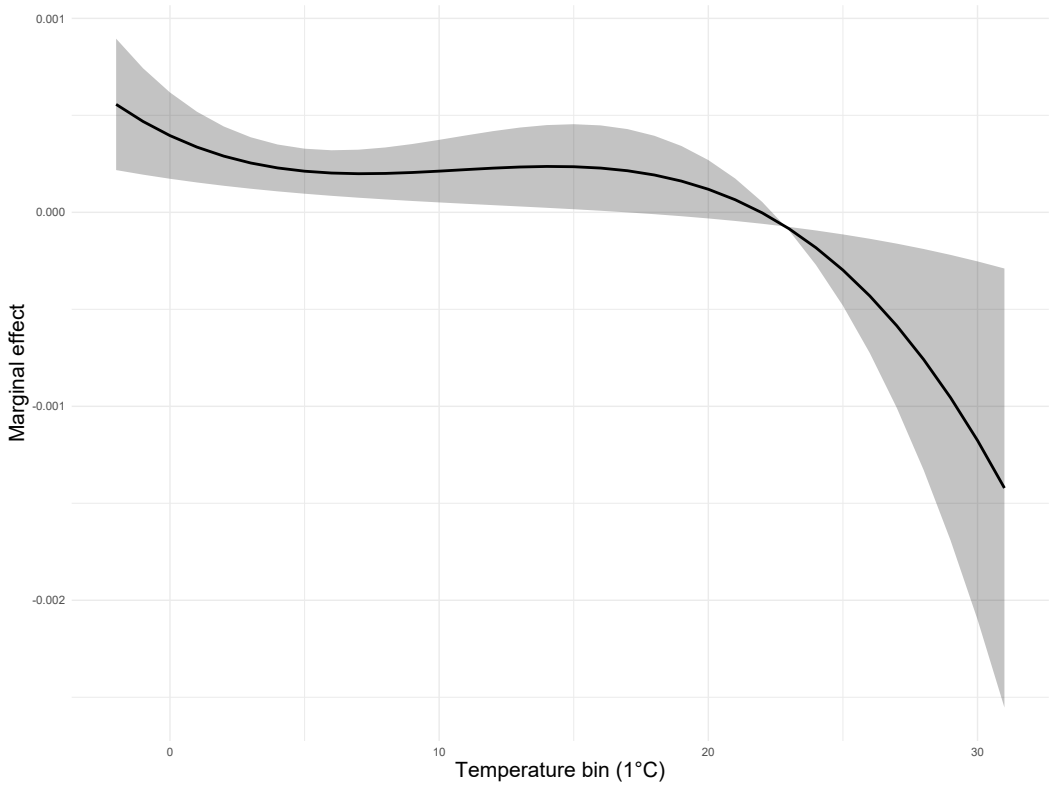

Figure 3: non-linear marginal effect (in %) of an additional day in the 1°C temperature bin on regional amenities computed from regression (12) with 95% confidence intervals. The regression is done with 95% winsorized bins [-2°C : 31°C] for 194.032 observations. For the simulations, I assume that below and above these thresholds, marginal effects remain constant.

In this dose-response function, estimates are for myopic households as my global approach does not allow to solve a fully dynamic migration decisions for 12674 locations. This approach with myopic households might underestimate negative marginal effects of low temperatures on regional amenities as shown in Rudik et al. (2022), which might explain why the marginal effect of low temperature on regional amenity is positive. As suggested in Albouy et al. (2016) for US households, we find a positive effect of moderate temperatures (around 18°C) on amenity value and large and increasing negative value of excess heat on the amenity value, consistent with observations on US data that households will pay more on the margin to avoid excess heat than cold. Finally, as amenity values are infered from migration flows, a drawback of this estima-

tion approach is that standard migration costs which are commensurable with changes in amenity values cannot be distinguished from the impossibility of migrating, such as administrative barriers, which are not. But I do not think that there is a reason to believe that it specifically biases a temperature bin over another.

3.3.2 Regional productivities

I follow a close procedure for regional productivities. The intuition behind this estimation is that an observed change in bilateral trade flows at the product level, controlling for changes in relative input costs, trade costs, and country and time fixed effects, as well as differences in annual distribution of daily mean temperatures between countries allows to identify nonlinear impacts of an additional day in a temperature bin on productivity value for the specific product. At equilibrium, expenditures of region n on industry k goods from region i write:

$$X_t^k(rs) = \left(\Gamma^k\right)^{-\theta^k} \frac{Z_t^k(s)(x_t^k(s))^{-\Theta^k}(\tau_t^k(rs))^{-\Theta^k}}{(P_t^k(r))^{\Theta^k}} X_t^k(r) \tag{13}$$

Normalizing by importer's own expenditures X_{rr}^k in industry k, using the expression for Z_{it}^k and taking the logarithm on both sides of the equation yields:

$$log\left(\frac{X_t^k(rs)}{X_t^k(rr)}\right) = \left[g(T_t(s);\zeta_Z^k) - g(T_t(r);\zeta_Z^k)\right] + log\left(\frac{\bar{Z}_t^k(s)}{\bar{Z}_t^k(r)}\right) - \theta^k log(\tau_t^k(rs)) - \theta^k log\left(\frac{x_t^k(s)}{x_t^k(r)}\right) \tag{14}$$

The left hand side is the ratio of expenditures on products of sector k from another region i to expenditures on products of sector k produced domestically. In equilibrium, it is equal to four terms. The first term on the right is the marginal difference in productivity between i and n due to climate impacts. Arbitrarily, I use a third-degree orthogonal polynomial smoothing across the regional annual distribution of daily 1°C binned mean temperatures. The second term is the difference in productivity due to non-weather fundamental differences. The third term are icerberg trade costs between

i and n. The fourth term is the relative price of inputs. For the empirical estimation, I combine BACI CEPII dataset for yearly sectoral international trade from 1995 to 2019 with World Bank population and GDP per country and sectors and Hersbach et al. (2020)'s climate reanalysis (ERA5) for annual distributions of daily mean surface temperatures at the country level. I process the climate reanalysis to aggregate it at the country level, weighting the 0.25° daily mean temperature observations with GHSL-POP population weights. I include tariffs in the fixed effects as data on tariffs (preferential and most-favoured nation) and non-tariffs trade costs τ from WITS database is very incomplete. I estimate the following regression with PPML:

$$log\left(\frac{X_t^k(rs)}{X_t^k(rr)}\right) = I_k * \left[g(T_t(s);\zeta_Z^k) - g(T_t(r);\zeta_Z^k)\right] + \zeta_X X_t^k + \rho_t^k + \phi_{ni}^k + \epsilon_{nit}^k \quad (15)$$

with ρ_t^k sector-year fixed effects and ϕ_{ni}^k importer-exporter-sector fixed effects. With X_t, I proxy for unobserved relative input costs with sectoral GDP per capita. Values for θ^k are taken from Caliendo and Parro (2015). Estimates are done at ISIC Rev.3 product level and the sector-specific response functions come from a regression where I interact the response function g with a set I_k of two sector dummy variables: agriculture and non-agriculture. The sector-specific regression is done on a distribution that is winsorized at 95%, so that the tails of the temperature distributions do not drive the results.

Variable	Coefficient	p-value
First-Degree Orthogonal Polynomial - Agriculture	1.57e-02	2.81e-08
First-Degree Orthogonal Polynomial - Non Agriculture	-2.02e-02	9.58e-02
Second-Degree Orthogonal Polynomial - Agriculture	-3.20e-02	0.00e+00
Second-Degree Orthogonal Polynomial - Non Agriculture	-2.22e-02	8.75e-04
Third-Degree Orthogonal Polynomial - Agriculture	-1.70e-02	0.00e+00
Third-Degree Orthogonal Polynomial - Non Agriculture	-2.07e-02	4.49e-03
Wald test, joint significance (Agriculture)	2.62e+02	0.00e+00
Wald test, joint significance (Non Agriculture)	3.01e+01	1.31e-06

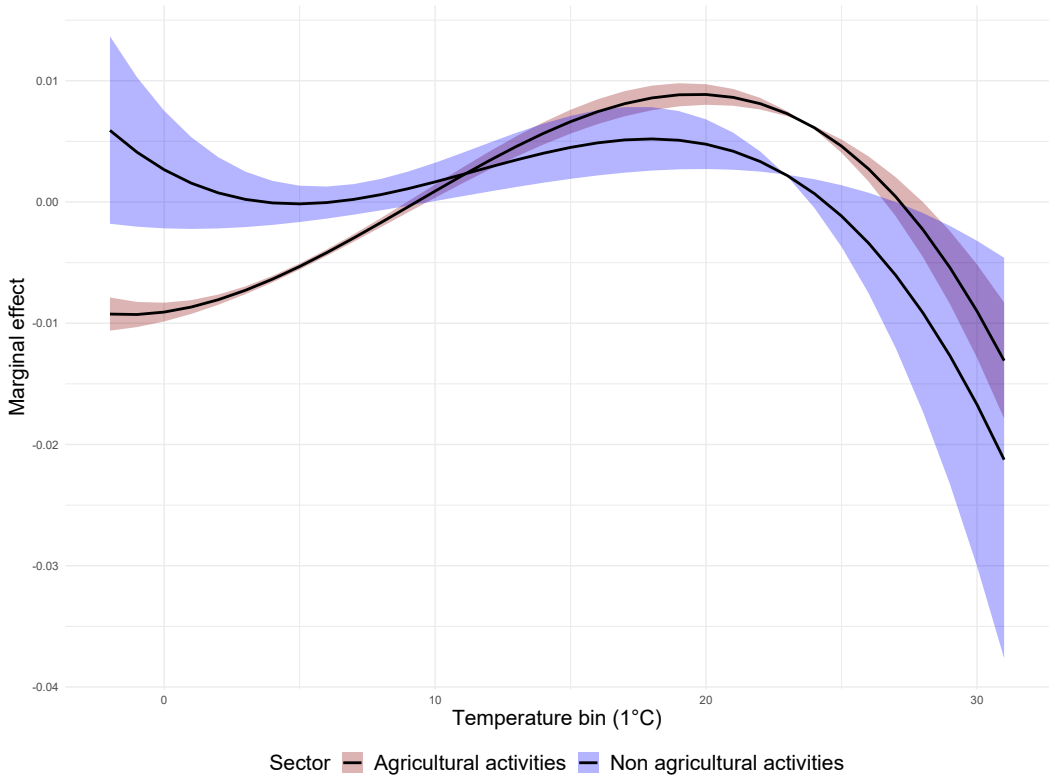

Figure 4: non-linear marginal effect of an additional day in the 1°C temperature bin on regional sectoral productivities computed from regression (12) with 95% confidence intervals and third-order orthogonal polynomials. The regression is done with 95% winsorized bins [-2°C : 31°C] for N=14.527.500 observations. For the simulations, I assume that below and above these thresholds, marginal effects remain constant.

As in Rudik et al. (2022), and consistent with previous literature (Burke et al., 2015), I find substantial evidence of negative impacts from elevated mean daily temperatures on sectoral productivity, affecting both agricultural and non-agricultural activities. Surprisingly, the marginal effects are more pronounced in non-agricultural sectors, even if confidence intervals are wider. Two factors may explain this finding. First, I employ a winsorizing technique at 31°C computed from the temperature distribution rather than an absolute threshold. This approach may wrongly reflect extreme temperature effects on agriculture, particularly at very high temperatures, due to a lack of sufficient observations. Second, since the analysis infers climate change impacts on sectoral productivity from trade flows, the estimates are on products and people

that are engaging in international trade. This might distort the estimated damage since agricultural sectors involved in export may be more competitive and adaptable, potentially underestimating the full extent of climate impacts. Related to this interpretation, a limitation of my estimation approach is that it does not allow for the estimation of dose-response functions for certain goods and services that are either untraded or non-tradable, such as transportation, education, healthcare, real estate, and local services like restaurants.

For agricultural sectors, I observe a bell-shaped relationship, with an optimal temperature for productivity around 20°C, consistent with results such as those of Conte et al. (2021). A key limitation in comparing my results to prior studies lies however in the use of daily average temperature bins rather than annual averages, which alters the form of temperature-productivity relationships. For non-agricultural sectors, I observe positive productivity effects for non-agricultural sectors on colder days (around and below 0°C). This result might be related to the differentiated effects identified by Burke et al. (2015), where wealthier countries—which might be disproportionately represented in trade data for non-agricultural products—demonstrate a greater capacity to adapt to lower temperatures. This distinction between rich and poor countries in their responses to temperature variations could explain the observed resilience of non-agricultural productivity to colder conditions.

4 Numerical results

4.1 Model resolution

Given the distribution of labor across markets $L_t \equiv \{L_t^k(r)\}_{r=1,k=0}^{N,K}$, location-industry fundamental productivities $Z_t \equiv \{Z_t^k(r)\}_{r=1,k=0}^{N,K}$, location-specific fundamental amenities $a_t \equiv \{a_t(r)\}_{r=1}^{N}$, I define a time-t momentary equilibrium as a vector of wages $w_t \equiv \{w_t(r)\}_{r=1}^{N}$ and aggregate price index $P_t \equiv \{P_t(r)\}_{r=1}^{N}$ satisfying equilibrium

conditions of the static multi-regional and multi-industry trade model. Let $\dot{\mu}_t \equiv \{\dot{\mu}_t(rs)\}_{r=1,s=1,t=1}^{N,N,\infty}$, $\dot{a}_t \equiv \{\dot{a}_t\}_{t=1}^{\infty}$, $\dot{u}_t \equiv \{\dot{u}_t\}_{t=1}^{\infty}$ be migration shares, amenities, and lifetime utilities changes respectively. Given an initial allocation of labor L_0^k, initial migration flows, initial sectoral trade flows, initial time-invariant exogenous fundamentals (migration costs, non-weather fundamental productivities and amenities, local structures), and a path of time-varying exogenous fundamentals (amenities, productivities, land uses and climate change), I define a sequential competitive equilibrium as a sequence of $\{L_t, \mu_t, u_t, w_t\}_{t=0}^{\infty}$ that solves the temporary equilibrium at each time t. Finally, I define a stationary equilibrium as a sequential competitive equilibrium such that the sequence $\{L_t, \mu_t, u_t, w_t\}_{t=0}^{\infty}$ is constant for every t. The intuition behind this approach is that observed data (migration flows, wages) are a good proxy for unobserved characteristics (migration costs, productivities) and that this observed data provides sufficient information to bypass the estimation of some fundamentals, for instance idiosyncratic non-weather regional amenities, to project future decisions by agents that include the distribution of this unobserved characteristics.

Some more datasets are needed at 1° gridded level for the simulations. I use 2015 GHSL-POP gridded population distribution and population-weighted country-level estimates of the share of employment in labour from World Bank. Exogeneous productivity paths are taken from SSP database and downscaled to 1° zone for SSP2 based on 2015 population coverage. For productivity paths, I take the mean of two modelling approaches for SSP2: OECD Env-Growth and IIASA. Population projections are taken from KC et al. (2024) SSP2 projections without migration. I use Conte et al. (2021) gridded sectoral initial bilateral sectoral trade flows. Agricultural and non-agricultural wages are computed using Kummu et al. (2018) gridded estimates of GDP per capita and population-weighted country-level estimates of the labour share of total income from ILOSTAT.

The initial bilateral migration flows are computed from Kummu et al. (2018) and

Abel and Cohen (2019): the gridded flows are constructed so that they match international migration flows, and internal migrations are built from within-country population-weighted net gridded migration stocks. There are two main issues with the modeling of migrations. First, when migration are fully dynamic, models cannot be solved at both global scale and fine resolution, while it would be useful to keep both characteristics. Applications with fully dynamic decisions (Caliendo et al., 2019; Balboni, 2019; Rudik et al., 2022) are for a subset of countries[4]. A second issue regarding migration dynamics is data availability at the right resolution: data is scarce, especially outside the USA. I keep a worldwide resolution (Cruz and Rossi-Hansberg, 2024) rather than restricting the analysis to the USA (Caliendo et al., 2019; Bilal and Rossi-Hansberg, 2023) or subset of countries for which rich migration data are available (Rudik et al., 2022). I reconstruct gridded migration flows from both international migration flows and gridded net migration stocks in a simplistic way that probably underestimate them but this first-order and fully explicit approximation relies on best-available gridded data products (Kummu et al., 2018; Abel and Cohen, 2019) and can be checked for robustness. Another avenue would be to invert the model to recover fundamentals such as migration costs, but it is also based on important modelling assumptions regarding the estimation of regional fundamental amenities.

4.2 Counterfactual climates and policies

To evaluate the aggregate welfare consequences of global warming and the welfare consequences of the biophysical channels, I compare at the gobal scale the present discounted value of regional utilities that are not idiosyncratic, namely,

$$W_0 = \sum_{r \in N} \sum_{t=0}^{\infty} \beta^t \dot{u}_{t+1}(r) = \sum_{r \in N} \sum_{t=0}^{\infty} \beta^t \dot{a}_{t+1}(r) \dot{y}_{t+1}(r) \tag{16}$$

[4]Recent advances include using deep neural networks (Azinovic et al., 2022) or perturbation approaches (Bilal and Rossi-Hansberg, 2023) could allow to keep both fully dynamic decisions and global 1° gridded approach. I leave work on these methodologies for future research.

In my approach, as in Cruz and Rossi-Hansberg (2024), I thus focus on changes in how individuals value the amenity and production characteristics of a location under changing climate. A drawback of this choice, discussed in Desmet et al. (2018), is that the welfare cost computed does not include two components: the mobility costs incurred to get there and the idiosyncratic preferences of individuals who live there.

I simulate the model in three alternative settings.

Simulation 1 - without climate change In this first benchmark simulation, I compute the distribution of future sectoral economic activities, population and trade flows that clear markets in each location at all future periods under the assumption that there is no climate change, i.e. no deviation in the annual distribution of daily mean temperatures in each location. This simulation is used as a baseline.

Simulation 2 - under biogeochemical SSP2-4.5 In the second simulation, I use bias-adjusted (Lange, 2019) and down-scaled projections from five CMIP6 Earth System Models forced with SSP2-RCP4.5 emissions under the assumption of fixed 2015 land use: GFDL-ESM4, IPSL-CM6A-LR, MPI-ESM1-2-HR, MRI-ESM2-0. More specifically, I construct a synthetic annual distribution of daily mean temperatures for each 1° location taking the average over five years. Thus, I can have a better proxy of the underlying climate distribution from which weather from a given year is drawn and capture some internal variability in climate, for instance due to El Niño. I compute the distribution of future sectoral economic activities, population and trade flows that clear markets in each location at all future periods under these nonlinear deformations in the annual distributions of daily mean temperatures in each location. The deviation between this simulation and the first one allows to compute the aggregate and distributional welfare impact of exogenous biogeochemical change along SSP2-4.5.

Simulation 3 - under both biogeochemical and biophysical SSP2-4.5 In the third simulation, I add the biophysical impacts driven by urban and agricultural

land demands to the exogenous biogeochemical projections, using the mapping between LULC changes and biophysical impacts that applies in this specific 1° Koppen Geiger climate zone at a given time period. The distribution of daily mean temperature in year t is the sum of exogeneous SSP2-4.5 scenarii and biophysical channels over each month within a year (net transitions to croplands) and over a year (transitions to urban areas). The comparison between this simulation and the second one allows to compute the aggregate and distributional welfare consequences of biophysical channels.

4.3 Benchmark biogeochemical climate impacts (SSP2-4.5)

First, I plot on the left graph of Figure (5) the 2100 future climate under SSP2-4.5 with respect to the 2015 distribution of temperatures, treating each location as a unit. The distortion of annual daily mean temperature distributions is less pronounced than in SSP5-8.5 or equivalent carbo-intensive pathways previously assessed (Cruz, 2021; Krusell and Smith Jr, 2022). Indeed, annual average temperature increases only from 15°C in 2015 to 17.3°C in 2100, i.e. a 2.3°C increase in mean annual surface temperature over our gridded locations of interest. On the right graph on Figure (5), I compare two shifts in the global intra-annual distribution of daily mean temperatures between 2015 and 2100. In red, I plot the difference in the frequency of a given mean daily temperature in the annual distribution using actual climate projections, i.e. I show how more frequent a given temperature is on average at the annual scale and over all locations in 2100 climate in comparison with 2015 initial climate conditions. In green, I apply a shape-preserving shift in annual mean to the 2015 distribution in blue on the left graph: I add to each mean temperature bin in 2015 the mean global annual difference between 2015 and 2100 in climate projections. This shift is approximate and illustrative as I round this shift again to match it to climate projections. These graphs show that even when aggregated to the global level, there are large changes in the shape of the intra-annual distribution of daily mean temperatures that are not

perfectly summarized by the annual mean deviation. This non-linearity is accounted for in our approach where we use the whole distribution of daily mean temperature to estimate climate impacts from the equilibrium conditions of the model and simulate their welfare consequences along our scenario.

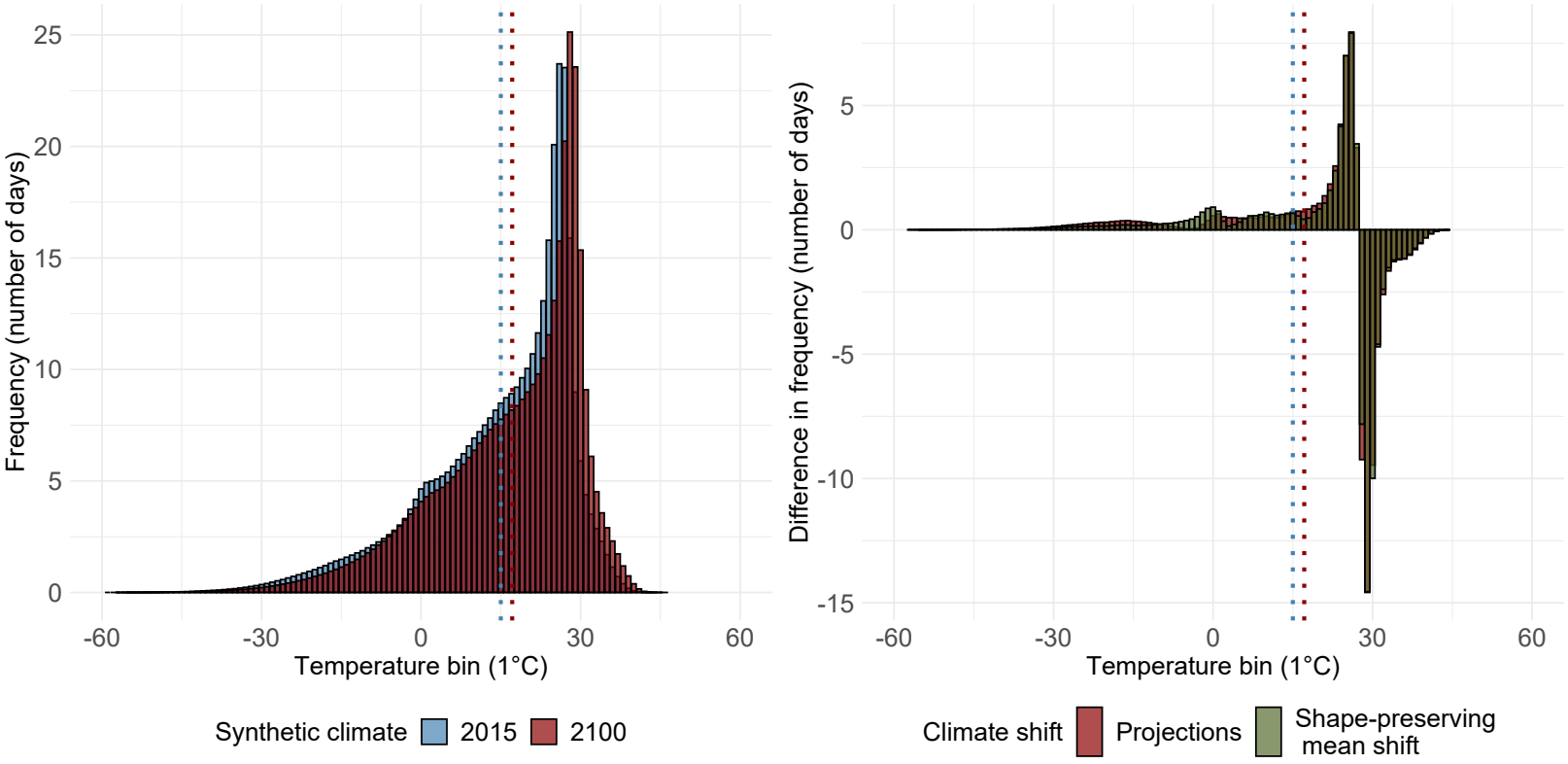

Figure 5: **Left** Synthetic global annual distributions of daily mean temperatures in 2015 (in blue) and 2100 (in red), under SSP2-4.5, for all gridded locations studied in the paper. Dotted lines represent average annual mean surface temperature. I treat each location as one unit. **Right** Shifts from 2015 to 2100 in the frequency of daily mean temperatures per temperature bin (in number of days) for climate projections (in red) and for a synthetic shape-preserving approximate annual mean shift where the annual mean increase observed between the two distributions 2015 and 2100 is added to each bin in the 2015 distribution.

I analyze both the aggregate and distributional welfare effects of climate change under the SSP2-4.5 scenario, focusing on locations where data is available (e.g. Libya is excluded due to missing data) and where population and economic activity were present in 2015. Thus, my analysis centers on the intensive margin of adaptation,

considering only existing areas and not the extensive margin—such as migration to currently uninhabited regions or the emergence of economic activity in areas with none in 2015. As there is no data on population and economic flows to reliably calibrate such predictions for these areas, I believe projections on this extensive margin would require a level of external model validity that is hard to achieve. In Figure 7, I present the distribution of changes in amenities and sectoral productivities across 12,674 gridded locations, using estimated dose-response functions.

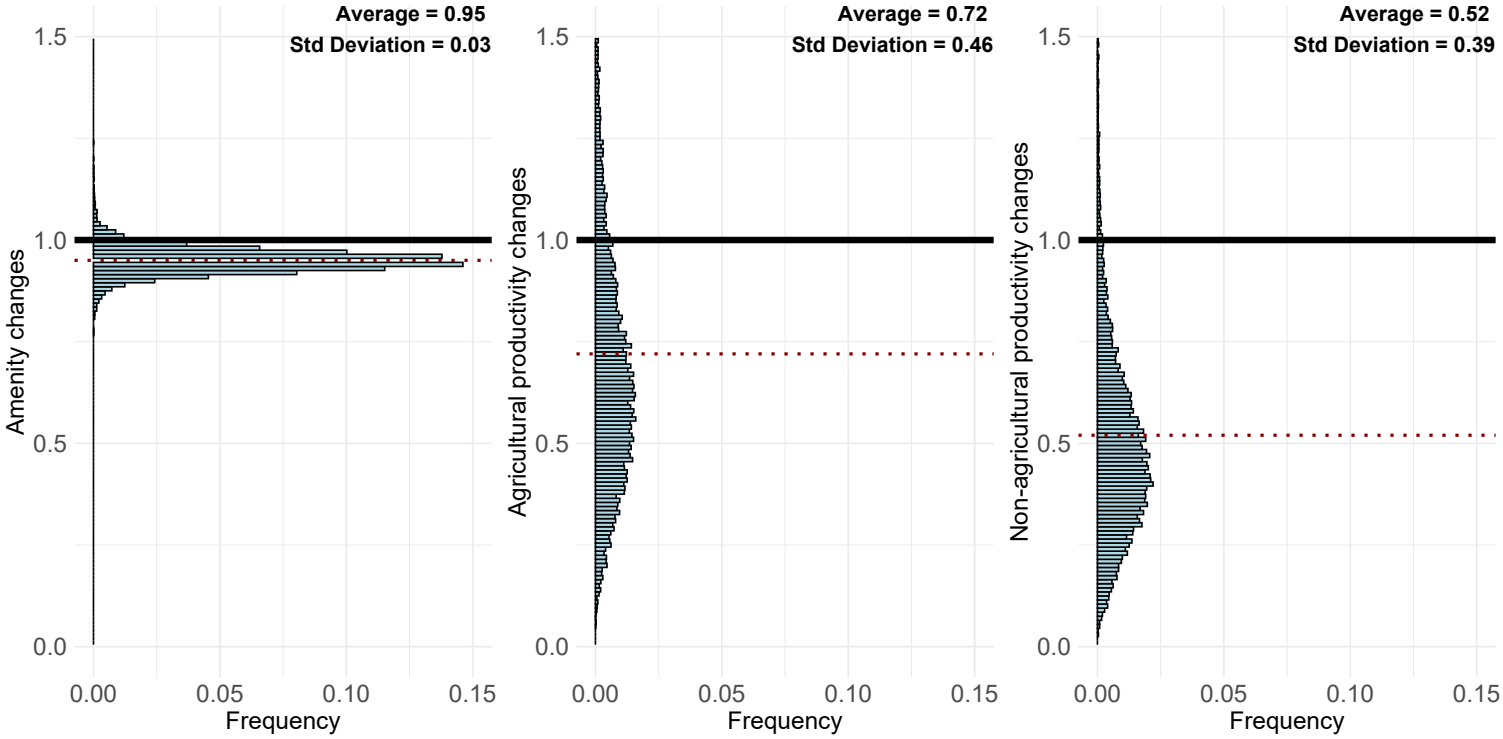

Figure 6: Ratio of amenity (left), agricultural productivity (middle), non-agricultural productivity (right) changes between scenario 2 with SSP2-4.5 forced with biogeochemical anthropogenic impacts and scenario 1 without climate change. For sectoral productivities, I winsorize the top of the distribution at 1.5 for illustration.

This graph yields three main conclusions. First, the average impact of climate change is negative for amenities and sectoral productivities. As in Cruz (2021) and as suggested by our dose-response functions, the marginal impact on amenity is one order of magnitude below the marginal nonlinear impact of temperatures on sectoral

productivities. Indeed, mean amenity changes are 5% with respect to baseline, while mean sectoral productivy changes are as large as 28% and 48% for agricultural and non-agricultural productivities. Second, in comparison with previous estimates yielding benefits from climate change for amenities and sectoral productivities in many locations, the impacts of climate change are negative for almost all locations when the entire intra-annual temperature distribution is considered. Even if some moderate daily mean temperatures have positive impacts on these variables in our dose-response functions, the aggregate effect is negative. Third, the impacts for sectoral productivities are much more dispersed than the impacts of climate change on amenities: most of the spatial heterogeneity will therefore come from these channels.

I then study how these changes in sectoral amenities and productivities translate into welfare impacts, once the adaptation of agents is taken into account. In Figure (7), I plot the distribution of changes in welfare in scenario 2 with biogeochemical climate change with respect to baseline scenario 1 without climate change.

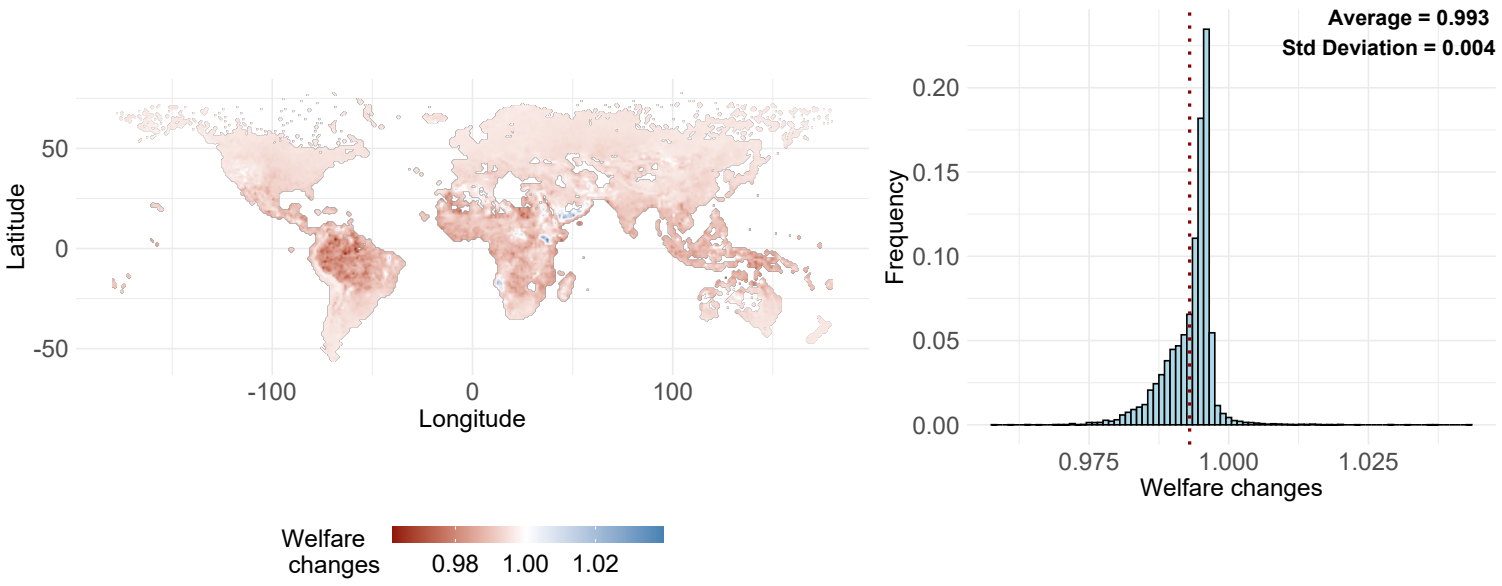

Figure 7: Ratio of welfare changes between scenario 2 with SSP2-4.5 climate impacts and counterfactual scenario 1 without climate change, plotted on a map with smoothed transitions between gridded locations (left) and on an histogram with the dotted average welfare change of 1% (right).

Figure (7) highlights two key findings. First, the mean welfare change under the SSP2-4.5 scenario is negative, with a 0.7% decline in welfare, equivalent to the 0.7% decrease estimated by Cruz (2021) for RCP6.0, despite RCP6.0 being a more carbon-intensive pathway. Second, with few exceptions driven by specific regional climates, such as the southern Arabian Peninsula, the marginal impact of climate change under SSP2-4.5 is negative across most regions. Contrary to previous estimates, I find no evidence of marginal benefits from climate change in northern locations. Since my analysis incorporates the intra-annual distribution of daily mean temperatures interacted with non-linear dose-response functions based on these distributions, the resulting welfare changes do not follow a simple isomorphic relationship to annual time-invariant temperature scalers that mimic polar amplification. The changes in annual temperature distributions are more complex than a uniform shift in the mean. These non-linear warming patterns, when combined with the non-linear response of welfare to temperature variations within the year, result in non-linear welfare impacts.

4.4 Counterfactual exogenous biophysical impacts (SSP2-4.5)

Building on the baseline estimates that include the biogeochemical impacts of climate change, I now assess the relative contribution of biophysical channels through LULC changes—the effects of albedo, evapotranspiration, and surface roughness. Figure 8 illustrates the distribution of welfare changes in scenario 3, which incorporates biophysical channels, relative to scenario 2, where only climate change impacts from the carbon cycle are considered without biophysical effects. These welfare changes are expressed as a fraction of the total change between scenarios 2 and 1, reflecting the standard climate impact estimates under SSP2-4.5, excluding biophysical channels. Thus, the estimates give the share the biophysical impacts represent in the standard biogeochemical estimates of the welfare impacts of climate change along SSP2-4.5.

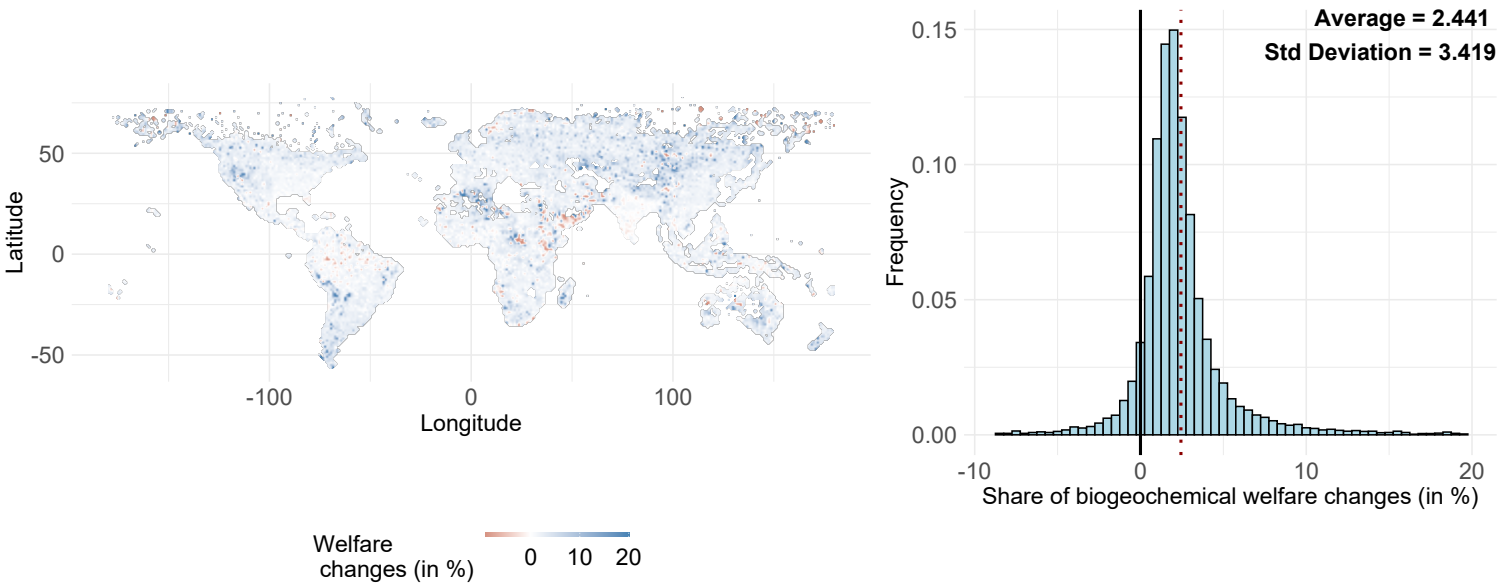

Figure 8: Share of welfare changes (in %) between scenario 3 with both SSP2-4.5 biogeochemical and biophysical channels and counterfactual scenario 2 without biophysical channels in the change between scenario 1 and scenario 2, plotted on a map with smoothed transitions between gridded locations (left) and on an histogram with the dotted average welfare change (right). The distribution is 98% winsorized.

Figure (8) provides two key insights. First, biophysical channels account for a non-negligible portion of the welfare impacts of climate change typically estimated from biogeochemical factors under SSP2-4.5, i.e. when temperature downscaling is assumed to be linear, time-invariant and exogenous to regional economic activities. Specifically, these regional biophysical processes, driven by LULC changes, contribute approximately 2.4% to the overall welfare impacts currently attributed to climate change. Regional economic activity does shape regional climate impacts. Second, the effects of these biophysical channels are predominantly negative across most regions.

Once I have retrieved the aggregate welfare impact of the biophysical channels, I estimate their distributional impacts with respect to standard biogeochemical climate impacts. In Figure (9), I plot the distribution of welfare impacts under biogeochemical impacts (left), under both biogeochemical and biophysical impacts (middle) , the distribution of the share of biophysical welfare impacts with respect to standard bio-

geochemical impacts (right) against the log of 2015 GDP per capita (ppp USD).

Figure 9: Distributional impacts of biogeochemical and biophysical channels along SSP2-4.5 **Left** Biogeochemical only with respect to no climate change (scenario 2 and scenario 1) **Middle** Both biogeochemical and biophysical impacts with respect to no climate change (scenario 3 and scenario 1). **Right** Deviation between scenario 2 and scenario 3 (scenario 3 and scenario 2). The red lines represent correlation, fitted using a linear regression model.

Figure (9) shows that the biogeochemical climate impacts are regressive, affecting more the poorest 2015 location. Indeed, a simple linear regression suggests that a 1% increase in GDP per capita yields a 0.1% decrease in welfare change with respect to the baseline simulation without climate impacts. Biophysical impacts further exacerbate the regressivity of biogeochemical impacts, by a 0.001% decrease in marginal welfare impacts for a 1% increase in 2015 GDP per capita. Thus, biophysical channels imply a 1% increase in the slope of the regressivity of standard biogeochemical climate impacts.

5 Discussion

As our understanding of the mechanisms through which human activities and climate impacts interact goes further, I investigate a mechanism qualitatively distinct from

the traditional biogeochemical one: the biophysical channel by which LULC changes bring regional climate impacts because of changes in albedo, evapotranspiration and soil roughness. While this mechanism might be negligible at a global scale in the first-order computation of the impacts of climate change, it does have heterogeneous regional effects that should be scrutinized carefully because they can cascade into large aggregate welfare effects and distributional consequences. In this paper, I quantify how and how much the regional biophysical channel of climate impacts driven by land use land cover changes matter. I first build a reduced-form representation of the regional biophysical feedbacks. Then, I leverage a dynamic quantitative spatial economic model applied to climate change with an explicit modelling of adaptation through trade, migration and changes in sectoral specialization. Furthermore, I estimate model-consistent dose-response functions of regional amenities and sectoral productivities to changes in the annual distribution of daily mean temperatures. Finally, I take the theoretical setting to the data at 1° gridded global scale. I solve the model with dynamic exact hat algebra and compare a baseline with forward-looking agents under 'middle-of-the-road' SSP2-4.5 without regional biophysical feedback to the counterfactuals with regional LULC changes and biophysical feedbacks. I compute the distributional and aggregate welfare impact for benchmark model and under counterfactual climates regarding LULC.

In conclusion, my analysis demonstrates that regional economic activity plays a significant role in shaping regional climate impacts. By incorporating biophysical channels into the assessment of SSP2-4.5, I find that these channels account for an additional 2.4% of the biogeochemical impacts on welfare, on average. The effects are unevenly distributed, influenced by both socioeconomic factors—such as urban land-use changes and transitions from shrublands or forests to croplands—and by shifting climate zones. Notably, the impacts of biophysical channels are predominantly negative across regions and, like biogeochemical effects, are regressive, disproportionately affecting lower-income regions based on 2015 income levels. In both scenarii of future climate

impacts, interacting intra-annual warming patterns with non-linear damage functions from temperature bins implies that nearly all regions will suffer from the impacts of climate change, with no significant benefits expected in the Northern Hemisphere.

A future direction, which is already underway for this paper, is to endogenize marginal deviations from SSP2-4.5 in land-use change. I use the exogenous MESSAGE-Globiom scenario SSP2-4.5 as a first approximation. But around this benchmark SSP2-4.5 from which I calibrate productivity and population exogenous paths, climate impacts and endogenous adaptation decisions (migration, sectoral specialization and trade) drive marginal changes in LULC changes in comparison with the standard MESSAGE-Globiom scenario. I could map marginal changes in the model input stemming from endogenous adaptation decisions in my quantitative spatial model to changes in model output around this scenario with a flexible statistical relationship, e.g. a surrogate model with gaussian processes (GP) to emulate the more complex land-use model. Alternative avenues could be taken, each with its limits. First, I could use reduced-form econometrics on historical data, but there is no exogenous variation to leverage, be it an instrument or a quasi-experimental setting. Panel fixed effect approaches (Chen et al., 2020) are affected by endogeneity and simultaneity as the authors have no control over the data-generating process. Second, I could build a complete dynamic model of land use changes including a market for crops, for land prices, etc., as well as assumptions about agricultural and urban policies. But the dynamic relation in the competition for land use would be computationally demanding and hard to calibrate at the global 1° gridded scale. This GP approach might be adapted for four main reasons. First, it allows me to map marginal deviations around an established exogenous scenario SSP2-4.5 building on robust land-use models. Second, I have control over the data-generating process, both exogenous scenario for drivers and mechanistic relations between variables of interest. Third, the GP is flexible: it is a non-parametric regression tool where I do not define a specific functional form to the input-output

mapping ex-ante and I can handle non-linear relations. Fourth, GP allows uncertainty quantification as they are probability distribution over a function space.

There are other limits to my approach. First, I should include other impacts, as land use land cover changes have large impacts on other planetary limits, for instance biodiversity. Second, I could estimate counterfactual policies to reduce the welfare cost of these biophysical channels, for instance zero net land take or irrigation policies (Braun and Schlenker, 2023). Finally, I would like to explore further impacts, for instance precipitation (Devaraju et al., 2015; Smith et al., 2023) and its interaction with temperature changes (e.g. wet bulbs). Water cycle indeed raises concerns not only because of deforestation (Grosset et al., 2023), but also following urbanization (Sui et al., 2024). These investigations are left for further research.

A Appendix

A.1 Migration in hat algebra

I write the change in bilateral migration flows in dynamic exact hat algebra. Starting from the initial equation for bilateral migration flows, I write the equation in time differences:

$$\dot{\mu}_{r,s,t+1} = \frac{\frac{u_{t+1}(s)^{1/\Omega} m(s)^{-1/\Omega}}{\sum_{n\in N} u_{t+1}(n)^{1/\Omega} m(n)^{-1/\Omega}}}{\frac{u_t(s)^{1/\Omega} m(s)^{-1/\Omega}}{\sum_{n\in N} u_t(n)^{1/\Omega} m(n)^{-1/\Omega}}} \tag{17}$$

Then, as migration costs are assumed to be time-invariant :

$$\dot{\mu}_{r,s,t+1} = \frac{\dot{u}_{t+1}(s)^{1/\Omega}}{\frac{\sum_{n\in N} u_{t+1}(n)^{1/\Omega} m(n)^{-1/\Omega}}{\sum_{n\in N} u_t(n)^{1/\Omega} m(n)^{-1/\Omega}}} \tag{18}$$

I have that:

$$\dot{\mu}_{r,s,t+1} = \frac{\dot{u}_{t+1}(s)^{1/\Omega}}{\frac{\sum_{n\in N} u_{t+1}(n)^{1/\Omega} m(n)^{-1/\Omega} \frac{u_t(n)^{1/\Omega} m(n)^{-1/\Omega}}{u_t(n)^{1/\Omega} m(n)^{-1/\Omega}}}{\sum_{n\in N} u_t(n)^{1/\Omega} m(n)^{-1/\Omega}}} \tag{19}$$

This yields the equation of interest.

A.2 Profit maximization

Profit in sector k (i.e. good i), location r, writes (symmetry between varieties ω):

$$\Pi_t^k(r) = p_t^k(r) z_t^k(r) L_t^k(r)^{\mu^k} H_t^k(r)^{1-\mu^k} - w_t(r) L_t^k(r) - R_t^k(r) H_t^k(r) \tag{20}$$

First-order conditions of profit maximization problem write:

$$\frac{\partial \Pi_t^k(r)}{\partial L_t^k(r)} = 0 \tag{21}$$

$$\frac{\partial \Pi_t^k(r)}{\partial H_t^k(r)} = 0 \tag{22}$$

Thus:

$$\mu^k p_t^k(r) z_t^k(r) L_t^k(r)^{\mu^k - 1} H_t^k(r)^{1-\mu^k} - w_t(r) = 0 \tag{23}$$

$$(1-\mu^k) p_t^k(r) z_t^k(r) L_t^k(r)^{\mu^k} H_t^k(r)^{-\mu^k} - R_t^k(r) = 0 \tag{24}$$

Replacing $p_t^k(r)$ yields:

$$R_t^k(r) H_t^k = \frac{1-\mu^k}{\mu^k} w_t(r) L_t^k \tag{25}$$

A.3 Prices and bilateral trade flows in exact hat algebra

Starting from the definition of prices (7), I write:

$$\dot{P}_{n,t+1}^k = \left(\sum_{l=1}^{N} \frac{Z_{l,t+1}^k [x_{l,t+1}^k \tau_{nl,t+1}^k]^{-\theta^k}}{\sum_{m=1}^{N} Z_{m,t}^k [x_{m,t}^k \tau_{nm,t}^k]^{-\theta^k}} \right)^{-1/\theta^k} \tag{26}$$

Multiplying and dividing each element in the summation just as what I have done for migration:

$$\dot{P}_{n,t+1}^k = \left(\sum_{l=1}^{N} \frac{Z_{l,t+1}^k [x_{l,t+1}^k \tau_{nl,t+1}^k]^{-\theta^k} \frac{Z_{l,t}^k [x_{l,t}^k \tau_{nl,t}^k]^{-\theta^k}}{Z_{l,t}^k [x_{l,t}^k \tau_{nl,t}^k]^{-\theta^k}}}{\sum_{m=1}^{N} Z_{m,t}^k [x_{m,t}^k \tau_{nm,t}^k]^{-\theta^k}} \right)^{-1/\theta^k} \tag{27}$$

Using trade flows from equation (10), I have the equation of interest (as trade costs are time invariant). Similarly for trade flows, I multiply and divide the numerator of (10) by $Z_{it}^k \left(x_{it}^k \tau_{nit}^k\right)^{-\Theta^k}$ and do the same for each element of the summation of the denominator:

$$\lambda_{nit+1}^k = \frac{Z_{it+1}^k \left(x_{it+1}^k \tau_{nit+1}^k\right)^{-\Theta^k} \frac{Z_{it}^k \left(x_{it}^k \tau_{nit}^k\right)^{-\Theta^k}}{Z_{it}^k \left(x_{it}^k \tau_{nit}^k\right)^{-\Theta^k}}}{\sum_l Z_{lt+1}^k \left(x_{lt+1}^k \tau_{nlt+1}^k\right)^{-\Theta^k} \frac{Z_{lt}^k \left(x_{lt}^k \tau_{nlt}^k\right)^{-\Theta^k}}{Z_{lt}^k \left(x_{lt}^k \tau_{nlt}^k\right)^{-\Theta^k}}} \tag{28}$$

Which yields:

$$\lambda_{nit+1}^{k} = \frac{\dot{Z}_{it+1}^{k}\left(\dot{x}_{it+1}^{k}\right)^{-\Theta^{k}} Z_{it}^{k}\left(x_{it}^{k}\tau_{nit}^{k}\right)^{-\Theta^{k}}}{\sum_{l}\dot{Z}_{lt+1}^{k}\left(\dot{x}_{lt+1}^{k}\right)^{-\Theta^{k}} Z_{lt}^{k}\left(x_{lt}^{k}\tau_{nlt}^{k}\right)^{-\Theta^{k}}} \tag{29}$$

Then, dividing by the sum:

$$\dot{\lambda}_{nit+1}^{k} = \frac{\dot{Z}_{it+1}^{k}\left(\dot{x}_{it+1}^{k}\right)^{-\Theta^{k}}}{\sum_{l}\lambda_{nlt}^{k}\dot{Z}_{lt+1}^{k}\left(\dot{x}_{lt+1}^{k}\right)^{-\Theta^{k}}} \tag{30}$$

A.4 Welfare

We study:

$$W_0 = \sum_{r\in N}\sum_{t=0}^{\infty}\beta^{t}\dot{u}_{t+1}(r) = \sum_{r\in N}\sum_{t=0}^{\infty}\beta^{t}\dot{a}_{t+1}(r)\dot{y}_{t+1}(r) \tag{31}$$

We have the equation for amenity changes. Changes in real income write:

$$\dot{y}_{t+1}(r) = \frac{\left(\sum_{k=1}^{K}(L_{t+1}^{k}(r)/L_{t+1}(r))w_{t+1}^{k}(r)\right)}{\left(\Pi_{k\in K}\dot{P}_{t}^{k}(r)^{\chi^{k}}\right)\left(\sum_{k=1}^{K}(L_{t}^{k}(r)/L_{t}(r))w_{t}^{k}(r)\right)} \tag{32}$$

A.5 Dose-response functions

At equilibrium:

$$\frac{\mu_{r,s,t}}{\mu_{r,r,t}} = \frac{u_t(s)^{1/\Omega}m(r,s)^{-1/\Omega}}{u_t(r)^{1/\Omega}m(r,r)^{-1/\Omega}} = \frac{\left(a_t(s)y_t(s)\right)^{1/\Omega}m(r,s)^{-1/\Omega}}{\left(a_t(r)y_t(r)\right)^{1/\Omega}m(r,r)^{-1/\Omega}} \tag{33}$$

Which yields:

$$log\left(\tfrac{\mu_{r,s,t}}{\mu_{r,r,t}}\right) = -\tfrac{\lambda}{\Omega}log\left(\tfrac{L_t(s)}{L_t(r)}\right) + \tfrac{1}{\Omega}log\left(\tfrac{\bar{a}_{t-1}(s)}{\bar{a}_{t-1}(r)}\right) + \tfrac{1}{\Omega}log(m(r,s)) + \tfrac{1}{\Omega}log\tfrac{y_t(s)}{y_t(r)} + \tfrac{1}{\Omega}\left(f(T_{s,t},\zeta_a) - f(T_{r,t},\zeta_a)\right) \tag{34}$$

A.6 Migration data

The key gap in our simulations is the matrix of intersectoral bilateral migration flows. First of all, I do no have data on sectoral migration at this grid level and at the global scale: I thus focus on bilateral migration flows without sector-specific mobility. Then, I combine a dataset $M^{inter}_{c1,c2}$ of 5-years international bilateral migration flows between c_1 (out) and c_2 (in) for each pair of N countries from 2010 to 2015 (Abel and Cohen, 2019) with gridded data of net migration stocks from 2010 to 2015 M^{intra}_{z} for each 1° gridded zone z from Kummu et al. (2018). The procedure, detailed in annex, has two steps. First, I compute the probability of international inflows and outflows for each zone times country based on net migration stocks and assign international migration flows based on these probabilities. Then, once international migration flows are deducted from net gridded migration stocks for each zone*country, I compute within-country migration flows between each region zone*country based on probability of intra-migration flows given gridded net migration stocks net of inter-country migration flows. I then aggregate the flow at 1° zone level. My procedure probably underestimates migration flows (i.e. overestimates migration costs) but I unfortunately do not have gridded births and deaths data to reconstruct migration flows à la Abel and Cohen (2019). For robustness, I run simulations with lower migration costs.

- Compute the share $s_{z,c,L2010}$ of each 1° zone z that is in country c based on 2010 population at level 0.1°. Compute the net migration stock $M^{intra}_{z,c} = s_{z,c,L2010} * M^{intra}_{z}$ of each pair (c,z) based on these population weights

- Normalize net migration stock at country c level for inflows
  $\bar{M}^{inflows}_{z,c} = M^{intra}_{z,c} + min_c(M^{intra}_{z,c})$
  which yields a probability of international inflows for each (c,z)
  $P^{inflows}_{z,c} = \bar{M}^{inflows}_{z,c} / sum_c(\bar{M}^{inflows}_{z,c})$

- Normalize net migration stock at country c level for outflows, i.e.:

$$\bar{M}_{z,c}^{outflows} = -\left(M_{z,c}^{intra} - max_c(M_{z,c}^{intra})\right) \tag{35}$$

, which yields a probability of international outflows for each (c,z):

$$P_{z,c}^{outflows} = \bar{M}_{z,c}^{outflows} / sum_c(\bar{M}_{z,c}^{outflows}) \tag{36}$$

- Assign bilateral international migration flows (in and out) for each country c to each zone z based on these probabilities to obtain (1) $MB_{z1,z2}$ the 1° bilateral matrix of international migration flows and (2) $M_{z,c}^{intra-net}$, i.e. stock of migration flows at gridded-country level net of international migration flows.

- For each zone z1 in c:

  1. If stock in z1 is positive, compute the probability of receiving internal flows from all other z2. Normalize net migration stock at country c level for inflows for all z2, i.e. $\bar{M}_{z2,c}^{inflows,net} = M_{z2,c}^{intra,net} + min_c(M_{z2,c}^{intra,net})$, which yields a probability of internal inflows for each (c,z1,z2), $P_{z2,c}^{inflows,net} = \bar{M}_{z2,c}^{inflows,net} / sum_{c-z1}(\bar{M}_{z2,c}^{inflows,net})$
  2. If stock in z1 is negative, compute the probability of sending internal flows to all other z2. Normalize net migration stock at country c level for inflows for all z2, i.e. $\bar{M}_{z2,c}^{inflows,net} = -(M_{z2,c}^{intra,net} - max_c(M_{z2,c}^{intra,net})$, which yields a probability of internal inflows for each (c,z1,z2), $P_{z2,c}^{outflows,net} = \bar{M}_{z2,c}^{outflows,net} / sum_{c-z1}(\bar{M}_{z2,c}^{outflows,net})$

- Add these internal flows to our matrix $MB_{z1,z2}$.

A.7 Algorithm

Algorithm. Solve period by period the sequential competitive equilibrium given an initial allocation $(L_0^k, w_0^k, \mu_{i,n,0}, \lambda_{i,n,0})$ and an anticipated convergent sequence of changes in fundamentals, $\{\dot{\Theta}_t\}_{t=0}^{\infty}$ (regional productivities and amenities affected by exogeneous biogeochemical climate impacts). without changes in LULC and biophysical channel. From this baseline scenario, I compute distributional and aggregate welfare impact of climate change along SSP2-4.5. The counterfactual [without climate change] is the same algorithm but with no climate impacts.

- Scenario 1: without climate impacts. In this baseline scenario, I compute the distribution of people and activity without future climate impacts.

- Scenario 2: with SSP2-4.5 climate impacts, without biophysical impacts. In this first counterfactual, I compute the distribution of people and activity and the aggregate and distributional welfare impacts of exogenous SSP2-4.5 without land use changes.

- Scenario 3: with SSP2-4.5 climate impacts and exogenous biophysical impacts. In this second counterfactual, I compute the distribution of people and activity and the aggregate and distributional welfare impacts of exogenous SSP2-4.5 with exogenous land use changes from MESSAGE-Globiom model.

Algorithm 1 Resolution

Inner loop solves the static equilibrium at each time period t. Outer loop computes path for fundamental variables given market clearing at each time t in each location r.

- Make an initial convergent (to 1 when T large) guess for the path of expected lifetime utilities expressed in time differences $\{\dot{u}^0_{r,t}\}^{T,N}_{t=0,r=1}$, where the superscript (0) indicates a guess.;

- While [outer loop] convergence criteria not met (tolerance, nb of loops)

  1. For all t, use $\{\dot{u}^{(0)}_{r,t}\}^{T,N}_{t=0,r=1}$ and $\{\mu_{r,n,0}\}^{N,N}_{r=1,n=1}$ to solve for the path of $\{\mu_{r,n,t}\}^{T,N,N}_{t=0,r=1,n=1}$.
  2. For all t, use equation for population dynamics, $\{\mu_{r,n,t}\}^{T,N,N}_{t=0,r=1,n=1}$,$\{L^k_{r,0}\}^{T,N,K}_{r=1,k=1}$ and SSP2 exogenous birth & death rates scenarii to get $\{L^k_{r,t}\}^{T,N,K}_{t=0,r=1,k=1}$
  3. Select climate scenario and recover the path of regional productivity and amenity changes in each r $\{\dot{Z}^k_t(r)\}^{T,N,K}_{t=0,r=1,k=1}$, $\{\dot{a}_t(r)\}^{T,N}_{t=0,r=1}$ from the scenario using estimated dose-response functions and exogenous productivity growth rates.
  4. For [inner loop] each period t > 0
     - Define a guess for wages $\{\dot{w}^{(0)}_{r,t+1}\}^{T,N}_{t=0,r=1}$
     - Obtain $\{\dot{x}^k_{r,t+1}\}^{N,K}_{r=1,k=1}$ using $\{L^k_t(r)\}^{N,K}_{r=1,k=1}$ and guess for $\{\dot{w}_{r,t+1}\}^{N}_{r=1}$.
     - Use $\{\dot{x}^k_{r,t+1}\}^{N,K}_{r=1,k=1}$, $\{\dot{Z}^k_t(r)\}^{N,K}_{r=1,k=1}$ and $\{\lambda^k_{rn,t}\}^{N,N,K}_{r=1,n=1,k=1}$ to obtain $\{\dot{P}^k_{r,t+1}\}^{N,K}_{r=1,k=1}$
     - Obtain $\{\lambda^k_{rn,t+1}\}^{N,N,K}_{r=1,n=1,k=1}$ from $\{\dot{P}^k_{r,t+1}\}^{N,K}_{r=1,k=1}$, $\{\dot{Z}^k_t(r)\}^{N,K}_{r=1,k=1}$, $\{\dot{x}^k_{r,t+1}\}^{N,K}_{r=1,k=1}$ and $\{\lambda^k_{rn,t}\}^{N,N,K}_{r=1,n=1,k=1}$
     - Compute $\{\dot{w}_{r,t+1}\}^{N}_{r=1}$ and check if market clears in each location
     - Update $\{\dot{w}^{(0)}_{r,t+1}\}^{N}_{r=1}$ if market does not clear
     - If market clears at t, compute aggregate price index $\{\dot{P}_{r,t+1}\}^{N}_{r=1}$ using fixed share of each good in worker's expenditure
  5. Repeat for each t to obtain at each period the momentary equilibrium and recover full paths of $\{\dot{w}_{n,t+1}\}^{T}_{t=0}$ and $\{\dot{P}_{r,t+1}\}^{T,N}_{t=0,r=1}$, which gives change in worker's real income.

- For each t, compute $\{\dot{u}_{t+1}(r)\}^{T,N}_{t=0,r=1}$ and change in worker's real income using $\{\dot{w}_{r,t+1}\}^{T,N}_{t=0,r=1}$ and $\{\dot{P}_{r,t+1}\}^{T,N}_{t=0,r=1}$. Check if $\{\dot{u}_{t+1}(r)\}^{T,N}_{t=0,r=1} \approx \{\dot{u}^{(0)}_{t+1}(r)\}^{T,N}_{t=0,r=1}$ according to convergence criterion. If not, go back to first step and update initial outer guess.

References

Abel, G. J. and J. E. Cohen (2019). Bilateral international migration flow estimates for 200 countries. *Scientific data 6*(1), 82.

Ahlfeldt, G. M., S. J. Redding, D. M. Sturm, and N. Wolf (2015). The economics of density: Evidence from the berlin wall. *Econometrica 83*(6), 2127–2189.

Albert, C., P. Bustos, and J. Ponticelli (2021). The effects of climate change on labor and capital reallocation. Technical report, National Bureau of Economic Research.

Albouy, D., W. Graf, R. Kellogg, and H. Wolff (2016). Climate amenities, climate change, and american quality of life. *Journal of the Association of Environmental and Resource Economists 3*(1), 205–246.

Alkama, R. and A. Cescatti (2016). Biophysical climate impacts of recent changes in global forest cover. *Science 351*(6273), 600–604.

Audretsch, D. B. and M. P. Feldman (1996). R&d spillovers and the geography of innovation and production. *The American economic review 86*(3), 630–640.

Azinovic, M., L. Gaegauf, and S. Scheidegger (2022). Deep equilibrium nets. *International Economic Review 63*(4), 1471–1525.

Balboni, C. A. (2019). *In harm's way? infrastructure investments and the persistence of coastal cities*. Ph. D. thesis, London School of Economics and Political Science.

Barrage, L. and W. Nordhaus (2024). Policies, projections, and the social cost of carbon: Results from the dice-2023 model. *Proceedings of the National Academy of Sciences 121*(13), e2312030121.

Beck, H. E., T. R. McVicar, N. Vergopolan, A. Berg, N. J. Lutsko, A. Dufour, Z. Zeng, X. Jiang, A. I. van Dijk, and D. G. Miralles (2023). High-resolution (1 km)

köppen-geiger maps for 1901–2099 based on constrained cmip6 projections. *Scientific data 10*(1), 724.

Bilal, A. and E. Rossi-Hansberg (2023). Anticipating climate change across the united states. Technical report, National Bureau of Economic Research.

Boysen, L. R., V. Brovkin, J. Pongratz, D. M. Lawrence, P. Lawrence, N. Vuichard, P. Peylin, S. Liddicoat, T. Hajima, Y. Zhang, et al. (2020). Global climate response to idealized deforestation in cmip6 models. *Biogeosciences 17*(22), 5615–5638.

Braun, T. and W. Schlenker (2023). Cooling externality of large-scale irrigation. Technical report, National Bureau of Economic Research.

Burke, M., S. M. Hsiang, and E. Miguel (2015). Global non-linear effect of temperature on economic production. *Nature 527*(7577), 235–239.

Caliendo, L., M. Dvorkin, and F. Parro (2019). Trade and labor market dynamics: General equilibrium analysis of the china trade shock. *Econometrica 87*(3), 741–835.

Caliendo, L. and F. Parro (2015). Estimates of the trade and welfare effects of nafta. *The Review of Economic Studies 82*(1), 1–44.

Chakraborty, T. and Y. Qian (2024). Urbanization exacerbates continental-to regional-scale warming. *One Earth*.

Chen, G., X. Li, X. Liu, Y. Chen, X. Liang, J. Leng, X. Xu, W. Liao, Y. Qiu, Q. Wu, et al. (2020). Global projections of future urban land expansion under shared socioeconomic pathways. *Nature communications 11*(1), 537.

Coeurdacier, N., F. Oswald, and M. Teignier (2022). Structural change, land use and urban expansion.

Conte, B., K. Desmet, D. K. Nagy, and E. Rossi-Hansberg (2021). Local sectoral specialization in a warming world. *Journal of Economic Geography 21*(4), 493–530.

Cruz, J.-L. (2021). Global warming and labor market reallocation. *Unpublished Manuscript*.

Cruz, J.-L. and E. Rossi-Hansberg (2024). The economic geography of global warming. *Review of Economic Studies 91*(2), 899–939.

Desmet, K., R. E. Kopp, S. A. Kulp, D. K. Nagy, M. Oppenheimer, E. Rossi-Hansberg, and B. H. Strauss (2018). Evaluating the economic cost of coastal flooding. Technical report, National Bureau of Economic Research.

Desmet, K., D. K. Nagy, and E. Rossi-Hansberg (2018). The geography of development. *Journal of Political Economy 126*(3), 903–983.

Desmet, K. and E. Rossi-Hansberg (2024). Climate change economics over time and space. *University of Chicago, Becker Friedman Institute for Economics Working Paper* (2024-25).

Devaraju, N., G. Bala, and A. Modak (2015). Effects of large-scale deforestation on precipitation in the monsoon regions: Remote versus local effects. *Proceedings of the National Academy of Sciences 112*(11), 3257–3262.

Duveiller, G., L. Caporaso, R. Abad-Viñas, L. Perugini, G. Grassi, A. Arneth, and A. Cescatti (2020). Local biophysical effects of land use and land cover change: towards an assessment tool for policy makers. *Land Use Policy 91*, 104382.

Duveiller, G., J. Hooker, and A. Cescatti (2018a). A dataset mapping the potential biophysical effects of vegetation cover change. *Scientific data 5*(1), 1–15.

Duveiller, G., J. Hooker, and A. Cescatti (2018b). The mark of vegetation change on earth's surface energy balance. *Nature communications 9*(1), 679.

Eaton, J. and S. Kortum (2002). Technology, geography, and trade. *Econometrica 70*(5), 1741–1779.

Eckert, F. and M. Peters (2022). Spatial structural change. Technical report, National Bureau of Economic Research.

Fernández-Villalverde, J., K. T. Gillingham, and S. Scheidegger (2024). Climate change through the lens of macroeconomic modeling. Technical report, National Bureau of Economic Research.

Fillon, R., M. Linsenmeier, and G. Wagner (2024). Climate shift uncertainty and economic damage. Technical report, working paper.

Georgescu, M., D. B. Lobell, and C. B. Field (2011). Direct climate effects of perennial bioenergy crops in the united states. *Proceedings of the National Academy of Sciences 108*(11), 4307–4312.

Grosset, F., A. Papp, and C. Taylor (2023). Rain follows the forest: Land use policy, climate change, and adaptation. *Climate Change, and Adaptation (December 1, 2023)*.

Henderson, J. V., B. Y. Jang, A. Storeygard, and D. N. Weil (2024). Climate change, population growth, and population pressure. Technical report, National Bureau of Economic Research.

Hersbach, H., B. Bell, P. Berrisford, S. Hirahara, A. Horányi, J. Muñoz-Sabater, J. Nicolas, C. Peubey, R. Radu, D. Schepers, et al. (2020). The era5 global reanalysis. *Quarterly Journal of the Royal Meteorological Society 146*(730), 1999–2049.

Hooker, J., G. Duveiller, and A. Cescatti (2018). A global dataset of air temperature derived from satellite remote sensing and weather stations. *Scientific data 5*(1), 1–11.

Huang, B., X. Hu, G.-A. Fuglstad, X. Zhou, W. Zhao, and F. Cherubini (2020). Predominant regional biophysical cooling from recent land cover changes in europe. *Nature communications 11*(1), 1066.

Hurtt, G. C., L. Chini, R. Sahajpal, S. Frolking, B. L. Bodirsky, K. Calvin, J. C. Doelman, J. Fisk, S. Fujimori, K. K. Goldewijk, et al. (2020). Harmonization of global land-use change and management for the period 850–2100 (luh2) for cmip6. *Geoscientific Model Development Discussions 2020*, 1–65.

KC, S., M. Dhakad, M. Potančoková, S. Adhikari, D. Yildiz, M. Mamolo, T. Sobotka, K. Zeman, G. Abel, W. Lutz, et al. (2024). Updating the shared socioeconomic pathways (ssps) global population and human capital projections.

Kleinman, B., E. Liu, and S. J. Redding (2023). Dynamic spatial general equilibrium. *Econometrica 91*(2), 385–424.

Krusell, P. and A. A. Smith Jr (2022). Climate change around the world.

Kummu, M., M. Taka, and J. H. Guillaume (2018). Gridded global datasets for gross domestic product and human development index over 1990–2015. *Scientific data 5*(1), 1–15.

Lange, S. (2019). Trend-preserving bias adjustment and statistical downscaling with isimip3basd (v1. 0). *Geoscientific Model Development 12*(7), 3055–3070.

Lawrence, D. M., G. C. Hurtt, A. Arneth, V. Brovkin, K. V. Calvin, A. D. Jones, C. D. Jones, P. J. Lawrence, N. de Noblet-Ducoudré, J. Pongratz, et al. (2016). The land use model intercomparison project (lumip) contribution to cmip6: rationale and experimental design. *Geoscientific Model Development 9*(9), 2973–2998.

Manoli, G., S. Fatichi, M. Schläpfer, K. Yu, T. W. Crowther, N. Meili, P. Burlando,

G. G. Katul, and E. Bou-Zeid (2019). Magnitude of urban heat islands largely explained by climate and population. *Nature 573*(7772), 55–60.

Masson-Delmotte, V., H. Pörtner, J. Skea, E. Buendía, P. Zhai, and D. Roberts (2019). Climate change and land. *IPCC Report*.

Michaels, G., F. Rauch, and S. J. Redding (2012). Urbanization and structural transformation. *The Quarterly Journal of Economics 127*(2), 535–586.

Nath, I. (2022). Climate change, the food problem, and the challenge of adaptation through sectoral reallocation.

Nordhaus, W. (2008). *A question of balance: Weighing the options on global warming policies*. Yale University Press.

Redding, S. J. and E. Rossi-Hansberg (2017). Quantitative spatial economics. *Annual Review of Economics 9*, 21–58.

Rudik, I., G. Lyn, W. Tan, and A. Ortiz-Bobea (2022). The economic effects of climate change in dynamic spatial equilibrium.

Santer, B. D., T. M. Wigley, M. E. Schlesinger, and J. F. Mitchell (1990). Developing climate scenarios from equilibrium gcm results.

Schlenker, W. and M. J. Roberts (2009). Nonlinear temperature effects indicate severe damages to us crop yields under climate change. *Proceedings of the National Academy of sciences 106*(37), 15594–15598.

Smith, C., J. Baker, and D. Spracklen (2023). Tropical deforestation causes large reductions in observed precipitation. *Nature 615*(7951), 270–275.

Sui, X., Z.-L. Yang, M. Shepherd, and D. Niyogi (2024). Global scale assessment of urban precipitation anomalies. *Proceedings of the National Academy of Sciences 121*(38), e2311496121.

Zhao, L., X. Lee, R. B. Smith, and K. Oleson (2014). Strong contributions of local background climate to urban heat islands. *Nature 511*(7508), 216–219.

Zhou, D., J. Xiao, S. Frolking, L. Zhang, and G. Zhou (2022). Urbanization contributes little to global warming but substantially intensifies local and regional land surface warming. *Earth's Future 10*(5), e2021EF002401.